AFOSR-TR-97-0469

REPORT DOCUMENTATION PAGE

Form Approved
OMB No. 0704-0188

1. AGENCY USE ONLY (Leave blank)	2. REPORT DATE	3. REPORT TYPE AND DATES COVERED
	31 Jan 1997	Final 1 Sep 93 - 31 Aug 1996

4. TITLE AND SUBTITLE
Broadband Seismology and the Detection and Verification of Underground Nuclear Explosions

5. FUNDING NUMBERS
PE 61102F
Proj 2309/AS
F49620-93-1-0498

6. AUTHOR(S)
Mark Andrew Tinker

7. PERFORMING ORGANIZATION NAME(S) AND ADDRESS(ES)
Dept of Geosciences
University of Arizona
Tucson AZ 85721
(PI: Prof Terry C. Wallace)

8. PERFORMING ORGANIZATION REPORT NUMBER
SASO # 83

9. SPONSORING/MONITORING AGENCY NAME(S) AND ADDRESS(ES)
AFOSR/NM
110 Duncan Ave
Bolling AFB DC 20332

10. SPONSORING/MONITORING AGENCY REPORT NUMBER
Monograph Series of Seismic Research #97-01

11. SUPPLEMENTARY NOTES

12a. DISTRIBUTION AVAILABILITY STATEMENT
APPROVED FOR PUBLIC RELEASE:
DISTRIBUTION UNLIMITED

12b. DISTRIBUTION CODE

13. ABSTRACT (Maximum 200 words)

The detection and identification of low yield explosions requires seismic stations at regional distances. However, because the regional wavefield propagates within the extremely heterogeneous crustal waveguide, the seismic waveforms are also very complicated. Therefore, it is necessary to have a solid understanding of how the phases used in regional discriminants develop within different tectonic regimes. Thus, the development of the seismic phases Pn and Lg, which compose the seismic discriminant Pn/Lg are evaluated.

The most fundamental discriminant is event location since 90% of all seismic sources occur too deep within the earth to be unnatural. France resumed its nuclear testing program and conducted 6 tests starting in Sept., 1995. Using teleseismic data, a joint hypocenter determination algorithm was used to determine the hypocenters of the 6 explosions.

One of the most stressing problems in monitoring a CTBT is the detection and location of small seismic events. Although seismic arrays have become the major tool for event location, sparse regional networks of 3-component broadband stations must also be used, and surface wavetrain information will improve location of small events.

14. SUBJECT TERMS	15. NUMBER OF PAGES
Seismology Nuclear test monitoring Seismic phase discriminants	66
	16. PRICE CODE

17. SECURITY CLASSIFICATION OF REPORT	18. SECURITY CLASSIFICATION OF THIS PAGE	19. SECURITY CLASSIFICATION OF ABSTRACT	20. LIMITATION OF ABSTRACT
UNCLASSIFIED	UNCLASSIFIED	UNCLASSIFIED	SAR

THIS REPORT IS CORRECT AS IS

PER: MARK TINKER

(520) 626-5062

UNIVERSITY OF ARIZONA

TUCSON, AZ.

BROADBAND SEISMOLOGY AND THE DETECTION AND VERIFICATION OF UNDERGROUND NUCLEAR EXPLOSIONS

by

Mark Andrew Tinker

TABLE OF CONTENTS

LIST OF ILLUSTRATIONS

LIST OF TABLES

ABSTRACT

On September 24, 1996, President Clinton signed the Comprehensive Test Ban Treaty (CTBT), which bans the testing of all nuclear weapons thereby limiting their future development. Seismology is the primary tool used for the detection and identification of underground explosions and thus, will play a key role in monitoring a CTBT.

The detection and identification of low yield explosions requires seismic stations at regional distances (<1500 km). However, because the regional wavefield propagates within the extremely heterogeneous crustal waveguide, the seismic waveforms are also very complicated. Therefore, it is necessary to have a solid understanding of how the phases used in regional discriminants develop within different tectonic regimes. Thus, the development of the seismic phases Pn and Lg, which compose the seismic discriminant Pn/Lg, within the western U.S. from the Non-Proliferation Experiment are evaluated.

The most fundamental discriminant is event location as 90% of all seismic sources occur too deep within the earth to be unnatural. France resumed its nuclear testing program after a four year moratorium and conducted six tests during a five month period starting in September of 1995. Using teleseismic data, a joint hypocenter determination algorithm was used to determine the hypocenters of these six explosions.

One of the most important problems in monitoring a CTBT is the detection and location of small seismic events. Although seismic arrays have become the central tool for event detection, in the context of a global monitoring treaty, there will be some dependence on sparse regional networks of three-component broadband seismic stations to detect low yield explosions. However, the full power of the data has not been utilized, namely using phases other than P and S. Therefore, the information in the surface wavetrain is used to improve the locations of small seismic events recorded on a sparse network in Bolivia. Finally, as a discrimination example in a complex region, P to S ratios are used to determine source parameters of the M_W 8.3 deep Bolivia earthquake.

CHAPTER 1

INTRODUCTION

HISTORICAL DEVELOPMENT OF A COMPREHENSIVE TEST BAN TREATY

The first nuclear explosion, codenamed TRINITY, was detonated on July 16, 1945, in a desert valley called Jornado del Muerto (walk of the dead) in central New Mexico. The Manhattan Project had come to fruition. Four years later, on August 29, 1949, the Soviets detonated "Joe-1," their first nuclear test. It was a copy of the plutonium implosion weapon dropped on Nagasaki built from stolen plans. The design was never put into production and was detonated solely as a demonstration of nuclear capability. Humans had discovered and unleashed the power of the atom.

Although the nuclear bomb was largely responsible for ending Japanese aggression in World War II, the arms race between the United States and the Soviet Union had begun, with both nations endorsing the philosophy that the best defense was an unstoppable offense. Nuclear testing, primarily atmospheric, climaxed in 1962 with 139 tests conducted by four countries (Fig. 1.1). This was largely in response to two factors: 1) the end of the 1958-1961 U.S. - Soviet moratorium, and 2) the upcoming Limited Nuclear Test Ban Treaty (LTBT). In the mid 1950s, concern was growing about stopping weapon development as well as the environmental impacts of radioactive fallout from atmospheric tests. This led to the development and signing of the LTBT in 1963. It was a trilateral agreement between the United States, Soviet Union, and Great Britain that prohibited nuclear testing in space, in the atmosphere, and under water. In fact, the key leaders of these three nations were in favor of a comprehensive ban. However, such a Comprehensive Test Ban Treaty (CTBT) would have to wait because seismology was perceived as inadequate for monitoring underground nuclear explosions.

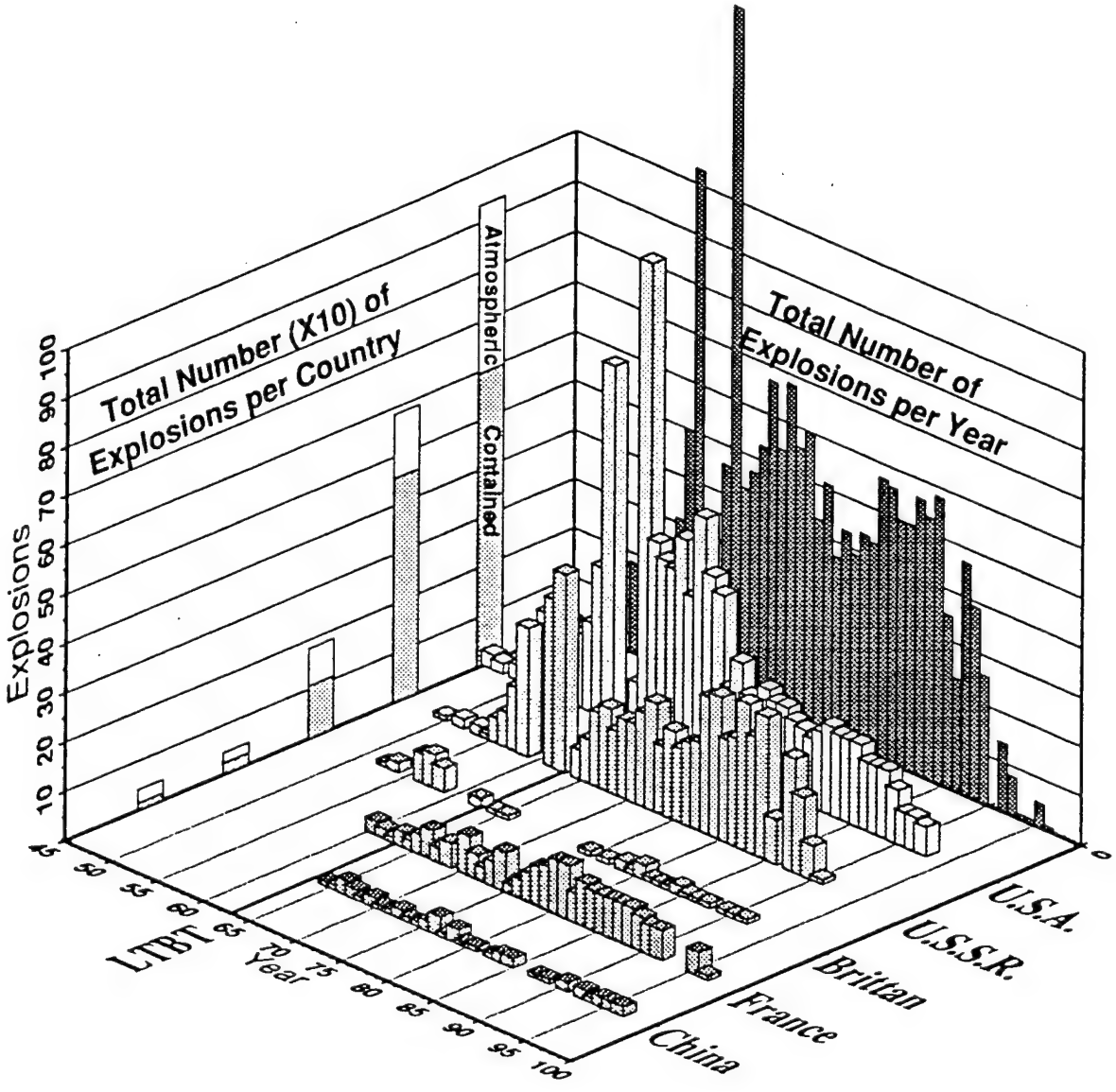

Figure1.1 A graph showing the total number of nuclear explosions detonated per year by country. The right side of the box represents the total number of nuclear explosions detonated each year irrespective of country. The left side of the box represents the total number of nuclear explosions detonated by a single country (times a factor of 10) separated according to whether or not the explosions was detonated in the atmosphere (before the LTBT) or underground.

At the time of negotiations, only one underground test had been conducted (RAINIER, at the Nevada Test Site in September, 1957). Furthermore, there were fundamental questions about seismology: 1) seismology as a science was not wide spread; only limited global data existed and then, only in analog form making rapid assessment impossible; and 2) seismic stations were few and far between; furthermore, they had a limited range of frequencies and low dynamic range. Thus, seismology could not support a major arms control agreement. This realization launched new efforts in instrumentation and seismological research. Project VELA began in 1959 under the Advanced Research Projects Agency of the United States Department of Defense. A portion of VELA included a plan by the United States Coast and Geodetic Survey to build a World-Wide Standard Seismograph Network (WWSSN). The network quickly grew to approximately 125 analog stations in 31 countries, and the science of seismology blossomed. Furthermore, a separate entity of seismology focusing on the detection and discrimination of underground nuclear explosions came into being. This was prompted by the need for such a discipline and was spurred on by the increasing amounts of data from the continuance of underground tests.

The Threshold Test Ban Treaty (TTBT) was signed on July 3, 1974. It restricts the yield of nuclear tests conducted by the United States and the Soviet Union to be less than 150 kt. This yield was based on the level of shaking caused in Las Vegas by testing at the Nevada Test Site. The TTBT posed a challenge to seismology that was based not on detection but yield determination. Seismically determined yields are a function of the statistical methods used to estimate the "magnitude" and are dependent on the material in which the test was conducted. Thus, during this time period, improvements in monitoring focussed on reducing the uncertainty in yield estimation. Nonetheless, a TTBT was the next logical step following a LTBT in terms of both global disarmament and the seismological state-of-the-art.

Towards the end of the twentieth century the Soviet Union collapsed which virtually ended the cold war between the super-powers. In subsequent SALT (Strategic Arms Limitation Treaty) agreements, the world's two largest nuclear stockpiles began to diminish. Furthermore, both the United States and the new countries from the defunct Soviet Union also strived to limit testing and the development of new generations of nuclear weapons (vertical proliferation). The logical conclusion of these efforts would finally have been a CTBT. This treaty would encompass as many nations (nuclear or non-nuclear) as possible. However, it was simultaneously discovered that Iraq was aggressively pursuing nuclear weapons development and the focus of a CTBT changed. Thus, seismology faces a new challenge. It must now address the spread and/or development of nuclear weapons within non-nuclear states (horizontal proliferation). This task is far more difficult than focusing on one nation, and it is equally if not more important given the diverse nationalities in pursuit of nuclear arms. Geographically, these areas include the Middle East, Pakistan, and North Korea, and it is very likely in the future there will be new areas of concern. Countries may also attempt to test outside their own geographical borders. Further, in the mid 1990s, both declared nuclear nations China and France actively pursed nuclear testing. Therefore, to enforce a CTBT, seismology must now monitor the entire planet, with the key question being, what is the smallest event that can be both detected and identified?

ENFORCING A CTBT: A SEISMOLOGICAL PERSPECTIVE

Modern seismic instrumentation is limited only by the noise levels in the earth. It has a large dynamic range, records the full spectrum of usable frequencies, and these high quality, broad band stations number in the hundreds. Furthermore, the digital age allows all seismic signals to be recorded digitally and sent anywhere in the world in a matter of seconds. Thus, the data is of high quality and accessible in near real-time. The science of

seismology in combination with the location and total number of stations is now the limiting factor .

As a monitoring tool, a seismic network must be able to both detect and identify the source of seismic signals. Unlike enforcing the TTBT, where a yield bordering at 150 kt is recorded by many stations due to its size (in other words, detection is not a problem), a CTBT must address the limits, or detection and identification thresholds, of a seismic network. Of course, the closer a station is to the source, the stronger and higher quality the signal. This is because the signal is strong enough to be well recorded above the background noise also recorded by seismometers. Furthermore, detection must occur at more than one station so that a location my be accurately estimated. Once a seismic event has been detected, it is then necessary to identify the source of the signal. Is it an earthquake, a legitimate chemical explosion, a rock burst, or a nuclear explosion? The smaller the event, the more unnatural and natural sources of seismicity from which it must be distinguished. For example, a fully tamped 10 kt explosion at NTS has a seismic magnitude of approximately 5.1. At Novaya Zemlya, Russia's nuclear test facility, and Lop Nor, China's nuclear test facility, this magnitude is slightly higher (≈5.2) due to the material properties in which the explosion is contained. There are an average of 7000 earthquakes a year that range in magnitude between 4.0 and 5.0. Further, there are tens of thousands more earthquakes per year with a magnitude less than 4.0 (Table 1.1). All of these events must be scrutinized in order to separate the potential suspect nuclear explosion from the legitimate sources. This is not a trivial task. As a good rule of thumb, a larger source is recorded at more stations. Therefore, there is a higher confidence in its location (latitude, longitude, depth, and origin time) as well as a higher confidence in its identification. It follows that detection is easier than identification. Thus, the smallest event that can be detected with reasonable confidence, known as a detection threshold, is usually

lower than an identification threshold. These thresholds can vary from region to region as a function of, for example, the number of recording stations, propagation characteristics, and source characteristics.

TABLE 1.1 Worldwide earthquake frequency by magnitude.

Seismic Magnitude	Number of Earthquakes per	
	Year	Day
4.5	2,300	6
4.0	7,100	19
3.5	19,000	52
3.0	68,000	186
2.5	209,000	572

Seismic Discriminants

Identifying a suspect event requires invoking what are called seismic discriminants. Seismic discriminants seek to exploit fundamental differences between earthquakes and explosions. For example, the most fundamental and useful seismic discriminant is the source depth. All underground nuclear explosions will be detonated within the uppermost crust; the deepest to date being 2.5 km. This is for two reasons. One, a depth greater than a few kilometers exceeds the ability of emplacement technology. Secondly, an underground explosion is detonated at a specific depth according to its predicted yield. This rubbelizes and collapses the overlying material so that all radioactive gasses are efficiently trapped. If there were to be a radioactive leak, not only is this a health risk, but it compromises any clandestine intentions since the radioactivity is readily detectable. Although determination of source depth can be difficult and have large uncertainties, 90% of all seismic events occur too deep to be unnatural, immediately reducing the number of events to be evaluated by other means. Further discrimination of the remaining 10% appeals to source phemonology.

Explosion sources in isotropic, homogeneous media produce compressive energy that radiates symmetrically outward in all directions about a point. Therefore, intuitively, an explosion should produce no shear energy. On the other hand, earthquake sources are shear dislocations along a plane. Thus, the P and S energy from an explosion should be different than that from an earthquake. Furthermore, single hole explosion source-time histories are impulsive, resulting in a higher corner frequency, whereas earthquake source durations are considerably longer yielding a lower corner frequency. In other words, seismic waves from explosions have more energy at higher frequencies for a given "size." For example, Figure 1.2 is a spectral comparison between the Non-Proliferation Experiment (NPE, a ≈1.1 kt chemical explosion) and an earthquake at approximately the same magnitude and distance. The corner frequency of the earthquake (0.8 Hz) is considerably lower than that of NPE. These two concepts of body wave energy and spectral content form the foundation for most discriminants.

With the need to monitor small events, discrimination has recently focused on regional (<1500 km) techniques. However, smaller earthquakes have shorter (more explosion-like) source durations. Thus, regional discriminants usually focus on P and S energy at higher frequencies by evaluating different frequency or spectral bands. Spectral discriminants are based on the differences in the spectral content of regional phases between explosions and earthquakes. Seismologists utilize this phenomenon to compare not only the spectral content of certain phases but also to compare the spectral energy of different frequency bands of the same phase. Spectral ratios compare the difference in energy at different frequency windows of the same phase. For example, the ratio of the Pn spectrum at 1-2 Hz to that at 2-4 Hz is denoted as Pn (1-2)/(2-4). Phase ratios compare the spectral energy between two phases of the same frequency window (Pn/Lg at 6-8 Hz), and cross spectral ratios compare different phases at different frequency windows (Pn (4-6)/Lg (2-4)).

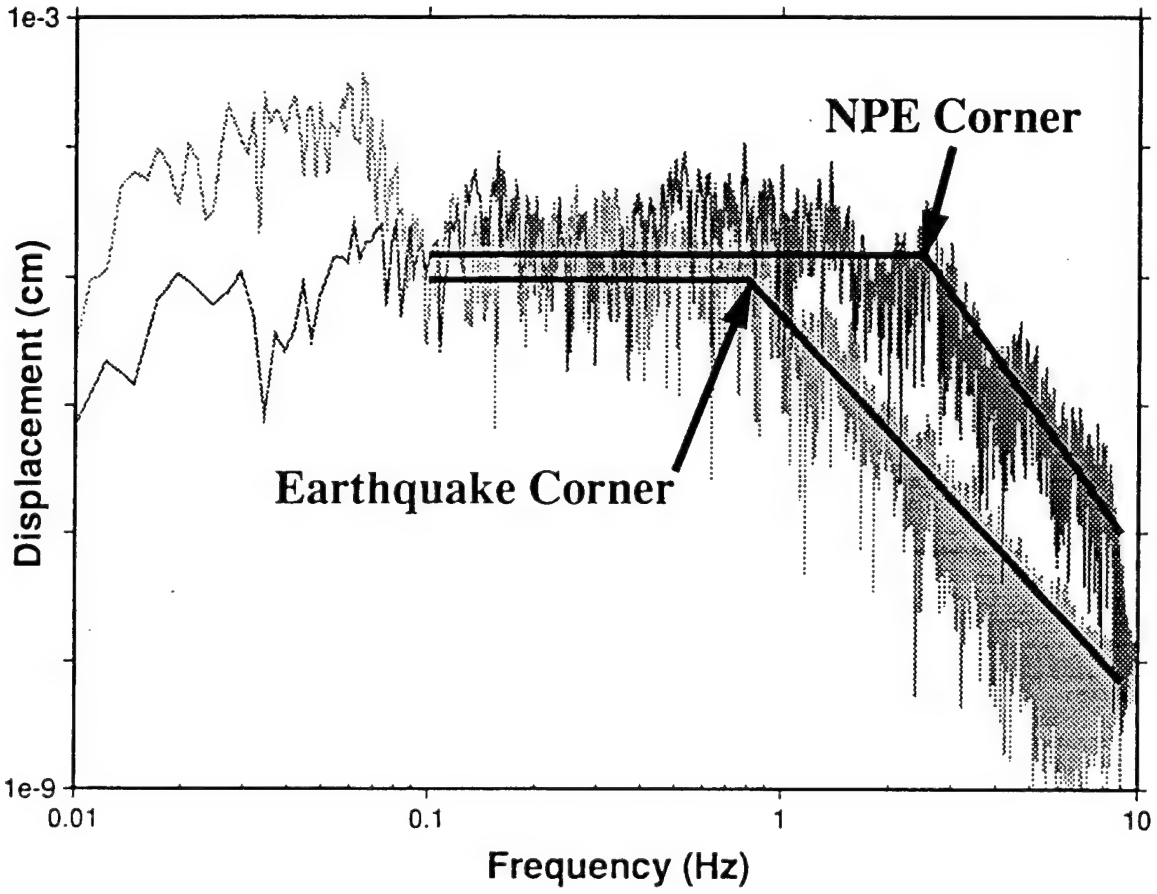

corner? →

Figure 1.2 A comparison of the spectral content of the Non-Proliferation Experiment (NPE) and a similar magnitude earthquake at approximately the same distance. NPE has a higher corner frequency (2.5 Hz) implying more high frequency energy while the earthquake has a lower corner frequency (0.8 Hz) and more long period energy (<0.1 Hz).

Regardless of the discriminant used, the ratio value is plotted compared to a field of other sources. Successful discriminants will separate explosion ratio values from earthquake ratio values.

International Data Center

To test the logistics of global monitoring, the Group of Scientific Experts Third Technical Test (GSETT-3) began full scale operations in January of 1995 at the prototype International Data Center (IDC) at the Advanced Research Projects Agency's (ARPA) Center for Monitoring Research in Arlington, Virginia. The purpose of this global seismological experiment was not only to develop rapid seismic monitoring for a CTBT as well as provide practical technical information for CTBT negotiators, but also to establish an international system that could evolve and adapt to support negotiated monitoring requirements. Thus, it would become an international data center geared towards global monitoring. The IDC incorporates four disciplines towards nuclear monitoring. After seismic, there is radionucleide, the detection of radioactive elements, hydroacoustic, and infrosound, which monitoring the world's oceans and atmosphere respectively for the propagation of energy within each medium that may be produced by a nuclear blast.

BROADBAND SEISMOLOGY

Broadband seismology plays a key role in the enforcement of a CTBT, aspects of which will be investigated in the following chapters. First, the effect of a complex region consisting of many geologic terrains on the seismic phases Pn and Lg will be evaluated. The is accomplished using 50 broadband seismic stations in the western United States that recorded the Non-Proliferation Experiment, a large (1 kt) chemical explosion. Subsequently, teleseismic locations are used to investigate France's nuclear testing facility in the Pacific by using a relative location algorithm to relocate 6 recent explosions. A regional location algorithm for broad band that incorporate surface waves is then explored.

Thus, the information from the full waveform is used while the dependence of phase travel times on a velocity structure is avoided. Finally, P to S ratios, analogous to most discriminants, are used to determine source parameters for aftershocks of a great, deep earthquake.

CHAPTER 2

REGIONAL PHASE DEVELOPMENT OF THE NON-PROLIFERATION EXPERIMENT WITHIN THE WESTERN UNITED STATES

INTRODUCTION

In September of 1996, a Comprehensive Test Ban Treaty (CTBT) was approved by the United Nations. This treaty will prohibit the testing of all nuclear weapons. Seismology is the primary tool used for the detection of underground explosions and thus, will play a key role in enforcing compliance of a CTBT. However, to effectively monitor a CTBT, seismologists must be able to confidently detect and identify low yield explosions. This requires seismic stations at regional distances (<1500 km). The regional wavefield propagates within the extremely heterogeneous crustal and upper mantle waveguide, and thus, the seismic waveforms are very complicated. Therefore, it is necessary to have a solid understanding of how the phases used in regional discriminants (Pn and Lg) develop within different tectonic regimes and change as a function of distance. Using the large number of explosions and earthquakes at the Nevada Test Site, Walter et al. (1995) performed a thorough analysis of various discriminants and source effects. They demonstrated the effectiveness of certain regional discriminants by showing a good separation between earthquake and explosion populations. However, only two stations were in operation long enough to record the sufficient number of events necessary for their analyses. Furthermore, since all of their events were located within NTS, it was not necessary to correct for path effects. Thus, they were constrained to only two station-source paths. This allowed them to determine the effect of the source in evaluating the effectiveness of each discriminant. Regional phases such as Pn and Pg are very dependent

on regionally varying lithospheric structure, therefore, the behavior of a regional discriminant may be very different for another area of the world. The identification of an unknown event recorded on a monitoring seismic array, if no prior explosion data exists for that array, would require comparing that event to other populations, such as the explosion and earthquake databases from the western United States. Without an understanding of path effects, such a comparison would be uncalibrated and non-definitive.

An experiment designed specifically to study the difference between chemical and nuclear explosions was detonated at the Nevada Test Site on September 22, 1993 (Denny, 1994; Hannon, 1994). This explosion, known as the Non-Proliferation Experiment (NPE), was a multi-fold experiment, including measurements of the hydrodynamic shock waves and free field particle velocities, accelerations, and stresses to measurements of electromagnetic pulses, gas samples, and atmospheric waves (Denny and Zucca, 1994). A large portion of the experiment focused on local and regional seismic surface measurements. The purpose of these include, 1) verifying possible differences between the seismic signature from a nuclear and chemical explosion, 2) investigating the evolution of regional seismic phases as they propagate across major tectonic provinces, and 3) determining the effects a change in geologic environments has on seismic discriminants.

The Southern Arizona Seismic Observatory at the University of Arizona participated in NPE by recording the explosion on an east-west, broad band seismic profile (Wallace et al., 1994). Ten broad band stations were installed on a line trending east from the Nevada Test Site to the Lawrence Livermore National Laboratory permanent seismic station KNB at Kanab, Utah. The purpose of this profile was to investigate the development of regional seismic phases and to explore the effects a change in geologic environments has on seismic discriminants. At the time of NPE, more than 30 permanent broad band stations were in operation in the western U.S. With the two portable broad band profiles (UA profile and

the profile operated by Lawrence Livermore National Lab (LLNL) and Cambridge University (McCormack et al., 1995)), NPE was the most seismically (broadband, 3-component) instrumented explosion in history. More than fifty regional broad band stations recorded the event, allowing not only for investigation of phase development at greater distances, but also as a function of azimuth (Fig. 2.1).

THE NON-PROLIFERATION EXPERIMENT

The United States Department of Energy conducted NPE in a large cylindrical chamber (15.2 meters in diameter by 5.5 meters in height) 390 meters under Rainier Mesa at NTS. The cylinder was filled with approximately 1.29 million kilograms of a 30/70 emulsion to ANFO (ammonium nitrate and fuel oil) blend (Denny and Zucca, 1994). This entire volume was detonated successfully at one minute past midnight on September 22, 1993, and recorded at over 50 broadband seismic stations.

The University of Arizona seismic profile consisted of 10 broad band STS-2 seismometers (frequency band 40 - 0.05 Hz), Reftek digitizers, and GPS clocks. Nine of the ten stations were operational during the explosion. The closest station to the shot point is 73 k; the remaining stations were located at approximately 20 km intervals beyond successive stations. Station KNB, the eastern most station in the profile, is 302 km from the shot point. The profile covers the transition between the Basin and Range and the Colorado Plateau (Station 1 is the furthest and Station 10 is the closest to the shot point, Figure 2.1). The remaining stations that recorded NPE are permanent stations operated by Incorporated Research Institutions in Seismology (IRIS)/Global Seismograph Network (GSN), Lawrence Livermore National Lab (LLNL), Sandia National Lab, TERRAScope, the Berkeley Digital Seismic Network (BDSN), and another portable broad band profile (trending 320° from NTS, 250km long) deployed by LLNL and Cambridge University, for a total of 50 stations. These stations range in distance from 73 km to 1029 km from NTS.

NPE PHASE DEVELOPMENT

Geologic setting

The southwestern U.S. is a tectonically complicated region, containing diverse and distinct geologic provinces. A large portion of the southwestern U.S. is occupied by the Basin and Range province, usually divided into northern and southern portions (Fig. 2.1). The northern Basin and Range has an average elevation approximately 1000 meters higher than the southern Basin and Range (Saltus and Thompson, 1995). The Basin and Range has a relatively thin crust and slower than average Pn velocities; the north has an average crustal thickness of approximately 30 km and an average Pn velocity of ≈7.8 km/sec, while the south has a more variable crustal thickness of 26 to 36 km and a slightly higher average Pn velocity of 7.8 - 8.0 km/sec (Hearn et al., 1991; for a complete review see Parsons, 1995). East of the Basin and Range is the Colorado Plateau, an area that has remained stable and intact during Tertiary extension and maintains an average elevation of ≈2km. The plateau has a slightly variable (≈15%) crustal thickness between 37 and 48 km (Parsons et al, 1996; Zandt et al. 1995), and Pn velocities range from 7.8 to 8.1 km/sec (Hearn et al., 1991; Beghoul et al., 1993). To the west of the Basin and Range is the Sierra Nevada. There has been considerable work done on the crustal structure of the Sierra Nevada, and the existence of a "crustal root" is still a subject of controversy. A recent experiment (Fliedner et al., 1996) modeled the Sierra Nevada with a small root (crustal thickness ≤ 43 km) and extremely low Pn velocities (7.6 to 7.8 km/sec) (Hearn et al., 1991). The thickest portion of the Sierra Nevada crust (≈43 km) is just south of the raypath between NTS and station CMB as shown in Figure 2.1 (Fliedner et al., 1996).

The Nevada Test Site (NTS) is located in the central Basin and Range of southern Nevada. Of the fifty stations that recorded NPE, approximately 26 are located within the Basin and Range (Fig. 2.1). The UA profile samples the Basin and Range (stations 10

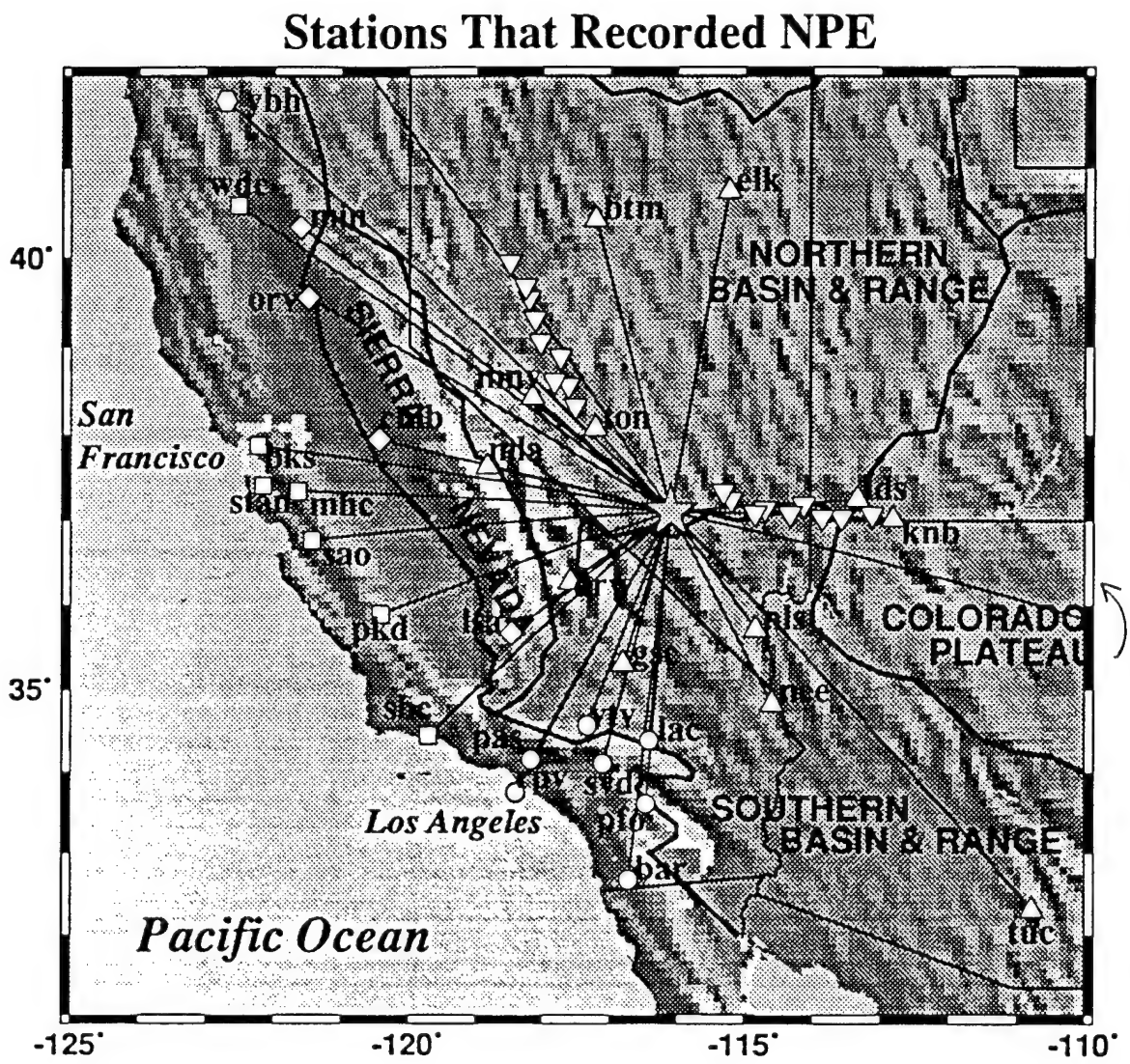

Figure 2.1 A map of the western U.S. showing the location of the permanent broadband stations that recorded NPE (star) as well as the location of the two portable profiles (inverted triangles). The symbol of the stations correspond to the geologic terrain or category in which they are located. Triangle (regular or inverted) = Basin and Range Terrain; Circle = Peninsular Ranges of southern California; Diamond = Sierra Nevada Terrain; Square = Pacific coast area on the side of the Great Valley from NTS; Hexagon = stations located greater than 750 km from NTS.

through 4) and the western most Colorado Plateau (stations 3, 1, LDS, KNB). Along the UA line, the 50-75 km wide transitional zone observed between the Basin and Range and the Colorado Plateau to the north and south, appears to be absent (Zandt et al., 1995). Although these four Colorado Plateau stations (stations 3, 1, LDS, KNB) are shown in Figure 2.1 as part of the Basin and Range, the following analysis does not ignore it is part of a different geologic province. The remaining stations are located in the Sierra Nevada terrain or three other categories that have been grouped by ray path according to the provinces traversed or distance (Fig. 2.1). Seven stations form the Peninsular Range group located in southern California (circles in Fig. 2.1). The Peninsular Ranges is a complex transition region separating North America from the Pacific. Stations located along the west coast of California compose the Pacific Coast group. Energy arriving at these stations has traversed the Basin and Range, the Sierra Nevada, and the Great Valley of California (squares in Fig. 2.1). The final group represents stations located at a distance greater than 750 km from NTS.

Pn and Pg Velocities and Structure Associated With the Two Portable Profiles

The University of Arizona seismic profile (UA) recorded NPE at 9 stations. Station 2 was not operational. However, a fortunate happenstance was that at the same distance and nearly the same azimuth was permanent station LDS, operated by Sandia National Laboratory. The vertical component waveforms from the entire UA profile are shown in Figure 2.2. The Pg velocity determined from a least squares fit is 6.04 km/sec. The apparent Pn velocity is a slow 7.6 km/sec, expected on the downward-dipping structure associated with the crust thickening to the east entering the Colorado Plateau. The shaded region in the record section outlines the Lg velocity window between 3.55 and 3.0 km/sec. Lg does not clearly emerge until Station 6 at 166 km. The same Lg behavior is observed for the Northwest profile (Figure 2.3). The apparent Pn velocity for the Northwest profile is

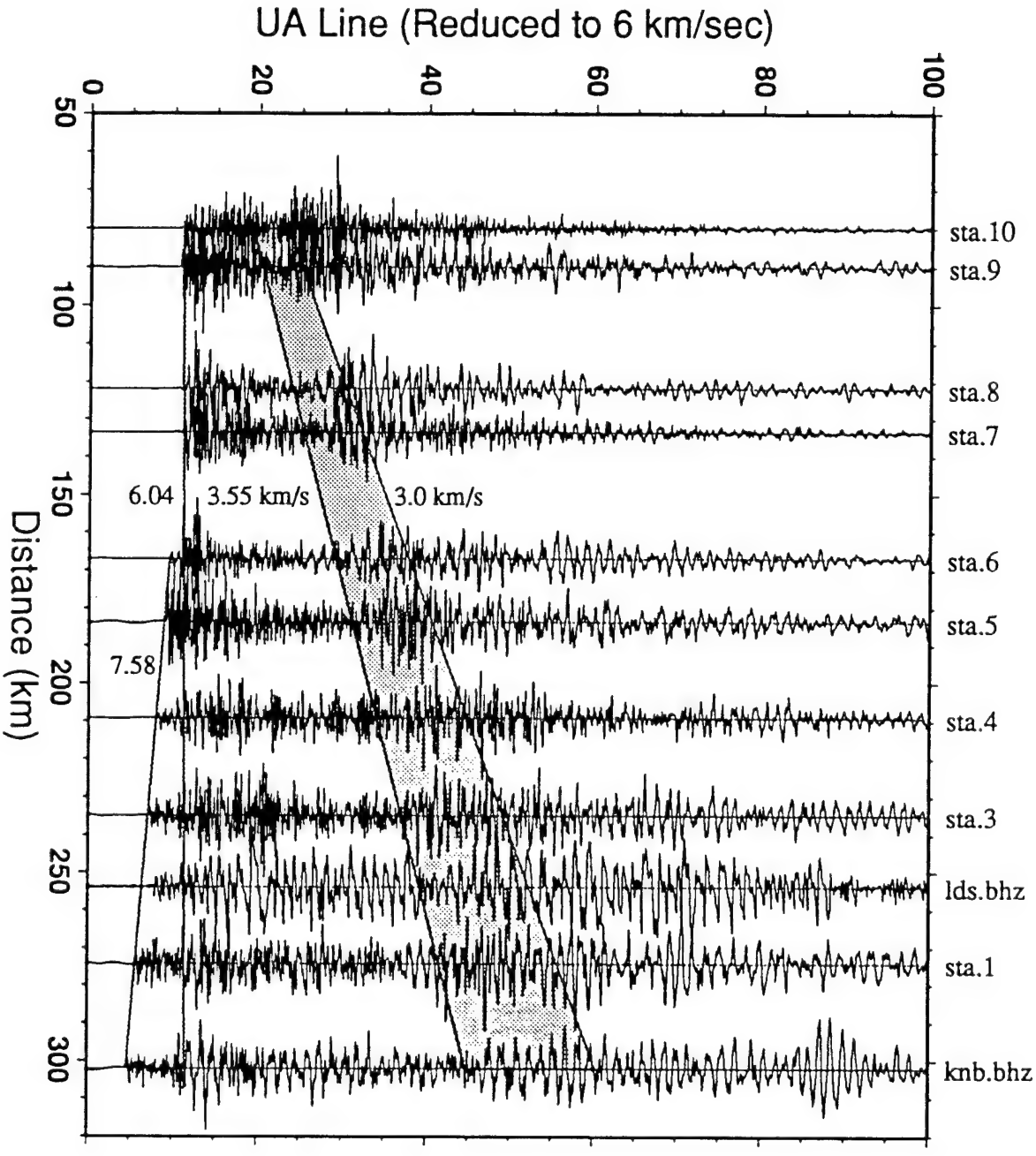

Figure 2.2 A travel time curve of NPE with a reduced velocity of 6 km/sec, recorded by the University of Arizona portable seismic profile. The apparent Pg velocity (6.04 km/sec) and the apparent Pn velocity (7.58 km/sec) were determined by a least squares fit to the data. The grey area between 3.55 and 3.0 km/sec represents the Lg velocity window.

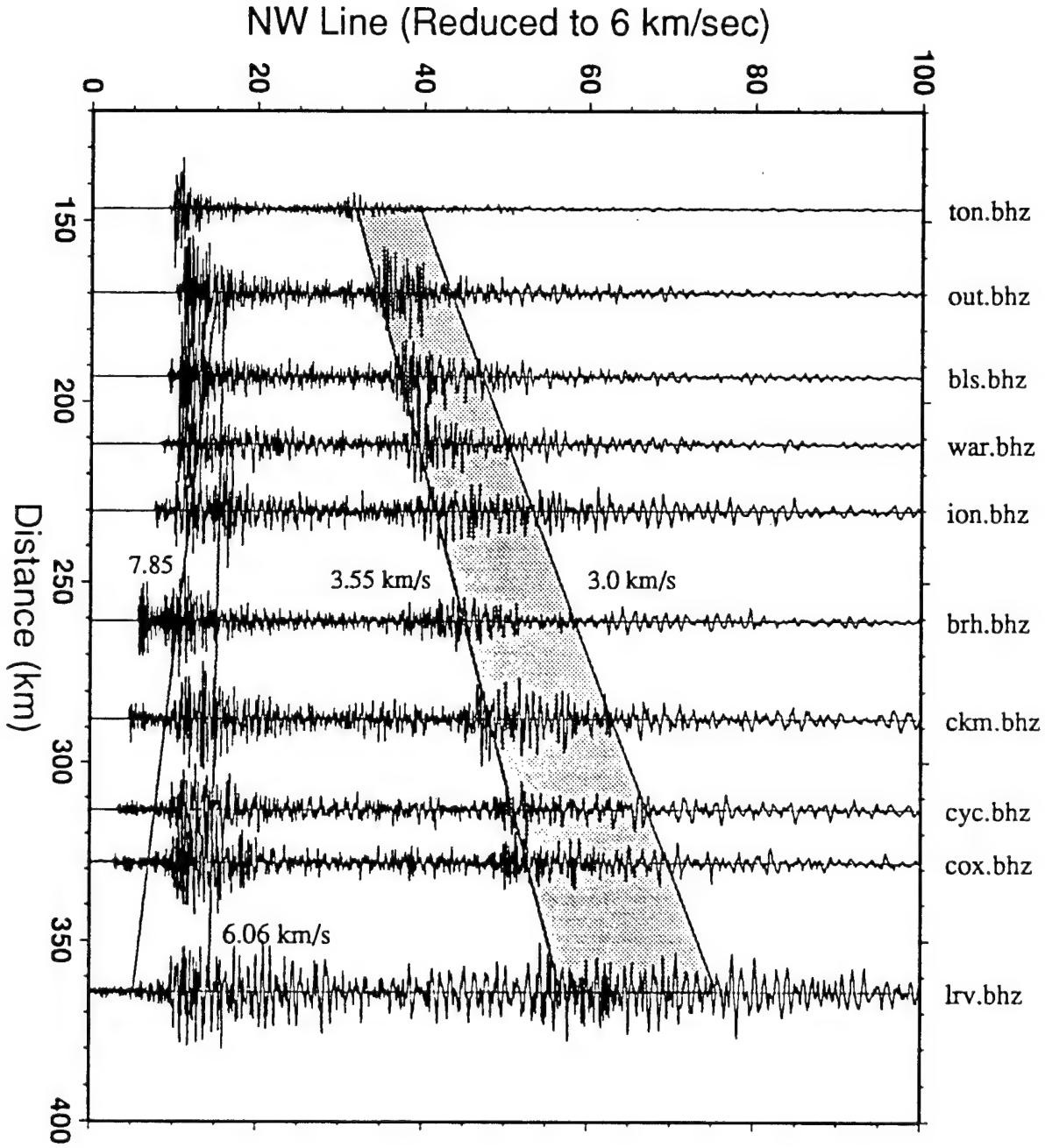

Figure 2.3 A travel time curve of NPE with a reduced velocity of 6 km/sec, recorded on the Northwest line (McCormack et al., 1994). The apparent Pg velocity (6.06 km/sec) and the apparent Pn velocity (7.85 km/sec) were determined by a least squares fit to the data. The grey area between 3.55 and 3.0 km/sec represents the Lg velocity window.

7.85 km/sec, and the Pg velocity of 6.06 km/sec (crustal average) is slower than the Pg velocity of the UA line.

Using a ray inversion code (RIC), we inverted the Pn and Pg times from both profiles and found the Moho dips downward to the east (UA line) and remains virtually horizontal to the northwest. We constrained the Moho to be flat and used a Pn velocity of 7.85 km/sec for the Northwest profile and 7.9 increasing to 8.0 km/sec for the UA profile. However, a flat Moho, or Moho represented by only one line segment, is not consistent with the seismic data or topography. Thus, to make the problem more realistic as well as to examine the non-uniqueness of the problem, we also inverted for a Moho structure consisting of 3 to 5 straight segments over the 400 km length of each model. This resulted in a crustal thickness under NTS of approximately 30 km. From NTS, out to 300 km on the UA line (the furthest distance sampled), the crust stepped downward to a thickness of 40 km. This is consistent with thicknesses determined from a receiver function analysis using the UA profile by Zandt et al. (1995). The Northwest line (nearly 370 km long) has a crust which is a reasonably constant thickness of approximately 30 km.

Lg and Pn Amplitudes and Attenuation

Lg is a complex crustal wavefield recorded on all three components of ground motion. It is usually interpreted as the superposition of a large number of higher mode Love and Rayleigh waves propagating in a crustal wave guide (Pomeroy, et al., 1982). Therefore, it is sensitive to both the vertical and lateral velocity variations within the earth's crust. To evaluate the phase Lg in the western U.S., we first attempted to remove the effects of attenuation and distance. Following the methodology of Chavez and Priestley (1986) we measured the distance decay of the spectral amplitudes of the Lg wave train recorded on the UA profile. We assumed that the Lg amplitude followed the relationship:

$$\log A(f,R) + \log R^{0.5} = \log S(f) - | (1.364f) / Q(f) | t \qquad (1)$$

where A is the spectral amplitude observed at a distance R, f is frequency, t is the travel time, S is the source term, and Q is the quality factor. This is the equation for a straight line in log(S) and 1/Q(f). We know R and t for each station. We then determined the amplitude (A) at a fixed frequency (f) for all the stations and solved for S and Q(f) using least-squares. In the above equation, the source term is the intercept and the Q term controls the slope. By measuring the spectral amplitudes over all frequencies, we obtained the source and Q spectra. Once Q is determined at each frequency, we then inverted for apparent Q as a function of frequency. This model does not consider attenuation due to scattering, thus, it provides only a measure of apparent Q, not intrinsic Q (Chavez and Priestley, 1986). For the UA line, we determined Q_{Lg}(vertical) = $388 f^{0.55}$ as compared to Q_{Lg}(vertical) = $217 f^{0.71}$ determined for the Northwest line by McCormack et al. (1994). This is reasonable given the greater structural integrity of the Colorado Plateau compared to that of the Basin and Range. This Q value was determined using stations east of and including Station 6, since Lg is not fully developed on stations 7 through 10. For the tangential component, we determined Q_{Lg}(tangential) = $362 f^{1.08}$ and McCormack et al. (1994) determined Q_{Lg}(tangential) = $180 f^{0.65}$ for the Northwest line. Finally, we determined Q for all the stations that recorded NPE in which we believe we could effectively convert to displacement. For these 43 stations in the multi-province southwestern U.S. we determined Q_{Lg}(vertical) = $238 f^{1.28}$ and Q_{Lg}(tangential) = $199 f^{1.16}$. These Q values are substantially lower than the 6 stations used from the UA line, because these Q values are averaged across the many geological provinces (Fig. 2.1) sampled by the travel path from NTS to the 43 stations .

There are large local variations in the amplitude of Pn across both profiles (Figs. 2.2 and 2.3). For example, there is a pronounced amplification of Pn energy at station 5 on the UA line (Fig. 2.2) and at station BRH, on the Northwest line (Fig. 2.3). A possible

explanation of this observation is the focusing and defocusing of Pn energy by undulations of the Moho (Zandt et al., 1995; Schultz et al. 1995). Starting with a simplified version of the crustal structure of the Northwest line (McCormack et al., 1994), we added three "undulations" to the structure of the Moho (Fig. 2.4). All three undulations (two negative, one positive) have an amplitude of only one kilometer. Using RIC, we traced on the Pn energy (Fig. 2.4). Even these small variations in the Moho can focus and defocus Pn energy over only tens of kilometers at the surface. Alternatively, Schultz et al. (1995) numerically model using reflectivity the amplified Pn at station BRH on the Northwest line. They show that when material contrasts are large enough, a local plane layered structure can result in significant Pn amplification. However, this site effect has a profound implication for lateral variations in structure since our stations have dense spacing (20 km); if the plane layered material contrasts were deep in the crust, then the Pn amplification could not be distinguished at one station over a seismic line with 20 km average spacing. Given what little is known of the geology at station BRH on the Northwest line, Schultz et al. (1995) produce amplified Pn arrivals using a low velocity volcanic layer either at the surface or a few hundred meters deep. Therefore, we prefer using topography on the Moho to explain amplified Pn arrivals that are not associated with local site effects.

Pn is not a simple geometric arrival, rather it is a combination of an effervescent wave and energy turning in the upper mantle. If it were a simple geometric ray, then the rays would turn in the upper mantle and be sensitive to the upper mantle velocity gradient. Therefore, both frequency dependent attenuation and geometrical spreading are affecting the Pn waveform with distance. We use the power spectral method of Chun et al. (1989) to determine a decay constant of the form $(\Delta^{-n(f)})$ (Δ = distance, f = frequency, n = decay constant). The displacement power spectrum of Pn ($P(f,\Delta)$) is related to a term containing

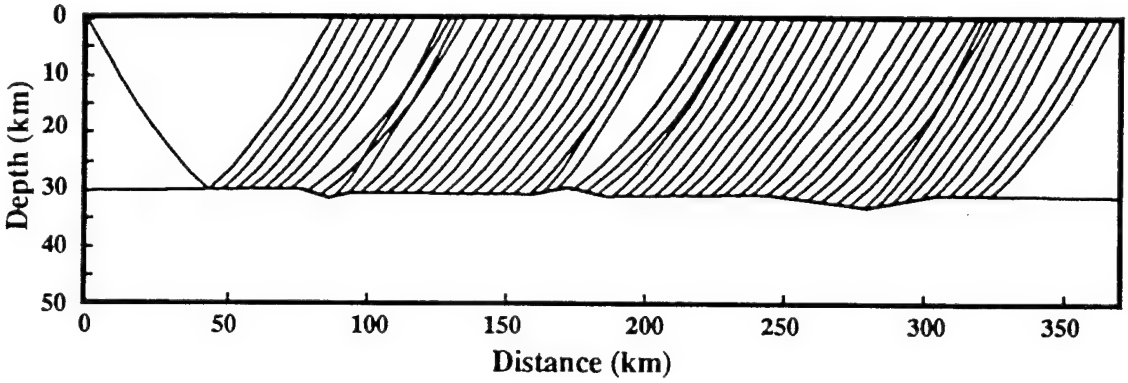

Figure 2.4 Aplot of Pn ray paths through a simplified crustal structure (from McCormack et al., 1994) of the Northwest line. Three one kilometer undulations were added in random locations. Notice the focusing and defocusing of Pn energy at the surface occurs over distances of tens of kilometers.

all the source and receiver function information (D(f)) and decay constant in the linear equation

$$\log P(f,\Delta) = D(f) - 2n(f) \log \Delta. \quad (2)$$

In a similar fashion to solving for Q, the slope of log P versus log Δ at a given frequency is -2n. Measurements over all the frequencies yields the decay constant "n" spectra. Fitting a line in a least-squares sense to the "n" spectrum yields the decay constant $\Delta^{-n(f)}$. McCormack et al. (1994) determined a decay constant of $\Delta^{-(1.84 + 0.48 f)}$ for the Northwest line. For the UA line we determined the Pn decay constant to be $\Delta^{-(1.34 + 0.19 f)}$ (1-10Hz). For the 38 stations in the southwestern U.S. in which the Pn phase could be confidently picked, we determined a Pn decay constant of $\Delta^{-(1.29 + 0.05 f)}$ for the frequency window of 1 - 6 Hz. At higher frequency bands, the range in data values was too large to effectively measure the decay.

SPECTRAL DISCRIMINANTS

Spectral discriminants quantify the differences in the spectral content of regional phases of explosions and earthquakes. The full seismic waveform from an explosion may have more energy at higher frequencies (>0.5 Hz) than an earthquake for a given "moment." For example, Figure 2.5 is a spectral comparison between NPE and an earthquake of approximately the same magnitude and distance. The corner frequency of the earthquake (0.8 Hz) is considerably lower than that of NPE. However, many NTS explosions show less high frequency energy than nearby earthquakes as shown in comparisons of spectral ratios (Taylor et al., 1988, Walter et al., 1995).

Phase discriminants (for example, Pn/Lg (6-8 Hz)) and cross-spectral discriminants (for example, Pn (4-6 Hz)/Lg (2-4 Hz)) seek to exploit the differences in P and S energy in explosions and earthquakes. Theoretically, explosions in a isotropic, homogeneous media produce compressive energy that radiates symmetrically outward in all directions about a

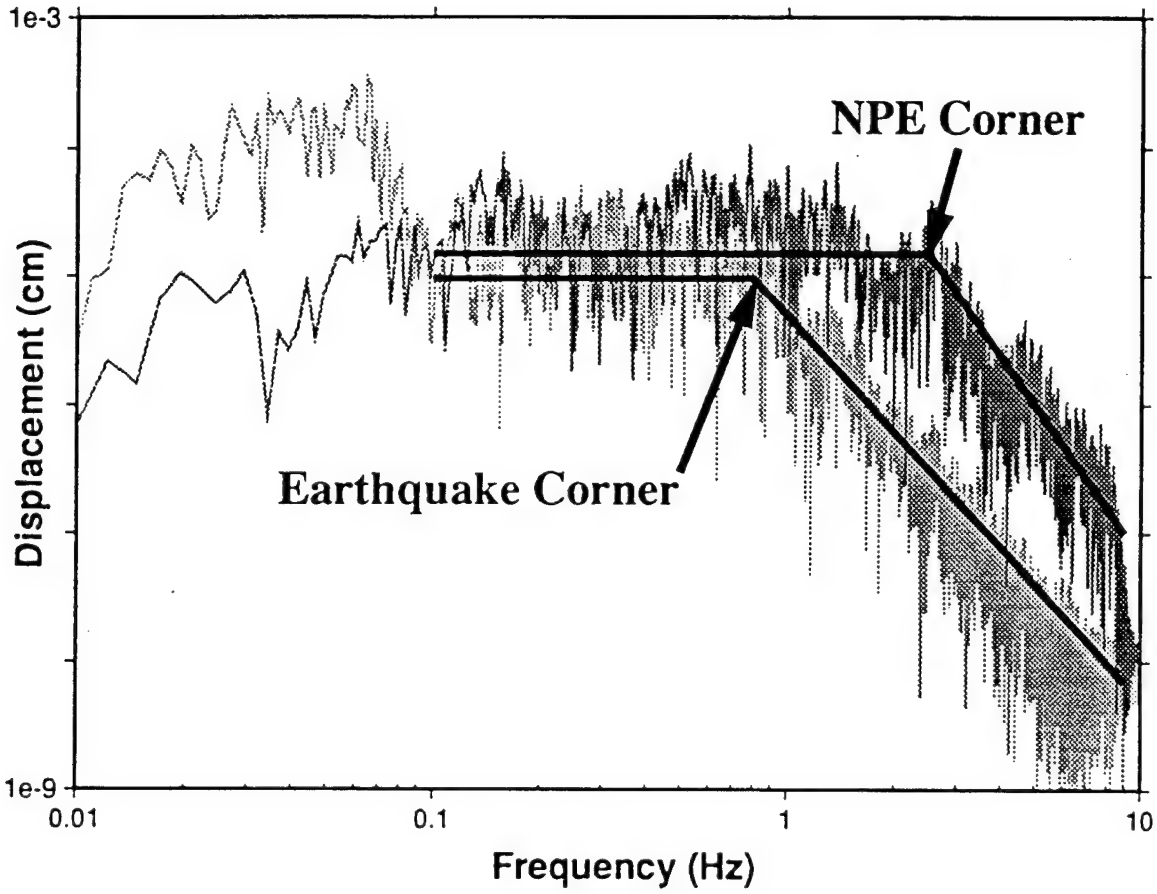

Figure 2.5 A comparison of the spectral content of the Non-Proliferation Experiment (NPE) and a similar magnitude earthquake at approximately the same distance. NPE has a higher corner frequency (2.5 Hz) implying more high frequency energy while the earthquake has a lower corner frequency (0.8 Hz) and more long period energy (<0.1 Hz).

point. Therefore, intuitively, an explosion should produce no S waves while having a strong P-wave first arrival. Earthquakes, on the other hand, are shear dislocations along a plane and produce strong S-wave energy. Although S-wave energy is commonly recorded from explosions, the P and S energy from an explosion is different than that from an earthquake. Thus, P/S ratios can discriminate between earthquakes and explosions, especially at higher frequencies (Walter et al., 1994). Although NPE was a chemical explosion, as discussed later, it is seismically indistinguishable from nuclear explosions. Thus, it is valid to use the expansive NPE data set to evaluate the effect of path on seismic discriminants.

With the advent of broadband seismology, discrimination techniques are able to incorporate wide spectral bands. Furthermore, using regional, high frequency phases (0.5-15 Hz) allows for the detection and possible discrimination to smaller magnitudes. For example, Taylor et al. (1989) and Walter et al. (1995) explored the effectiveness of various spectral ratio discriminants for numerous earthquakes and explosions located at the NTS and recorded on the Lawrence Livermore National Laboratory (LLNL) seismic network (4 stations). However, any technique that incorporates regional phases such as Lg, Pg, and Pn also requires an understanding of path effects (propagation through different geologic terrains) and distance dependence. Walter et al. (1995) explored the effect of source medium properties on spectral ratio performance since the source-station paths from the multiple sources at NTS were virtually the same for each of the two LLNL stations they used (MNV, KNB). They found that the source medium properties of gas porosity, strength, and depth significantly affected the Pg/Lg and spectral ratio discriminants.

To effectively monitor a Comprehensive Test Ban Treaty, a thorough understanding of both source and path effects on the applied discriminant is paramount if the discriminant is to be transportable, since most other areas of the world will not have the number of events

or stations found in the western U.S. with which to calibrate discriminants. With the large number of stations that recorded NPE, we can examine the effect of different terrains on spectral ratios. We first explore the spectral ratios of Lg/Lg and Pn/Pn to ascertain the contribution of each towards the phase ratio Pn/Lg.

Lg/Lg

As a discriminant, Lg is usually measured in a frequency window between 0.5 to 10 Hz. After removing the effects of distance and attenuation, we discovered that many of the Lg/Lg ratios as a function of distance exhibit scatter. For example, in Figure 2.6 there is a plot of the spectral ratio Lg (4-6)/(2-4) as a function of distance. Although this ratio is not commonly used in discrimination literature, it effectively demonstrates the following; the observed scatter is a function of both the geologic terrain or region in which the station is located in some sort of combination with the path traveled. The scatter is limited to about one order of magnitude. Thus, using Lg in a discriminant would influence the separation observed between earthquakes and explosions based on what station was used. The horizontal lines in the ratio value vs. distance plot in Figure 2.6 represent the average and one standard deviation of the mean of the ratio values of all stations less than 600 km away from NTS. Shown on the map in Figure 2.6 are the stations corresponding to the ratio values greater than one standard deviation (red triangle); greater than the average (light red circles); less than the average (light blue circles); and less than one standard deviation (blue triangles). Clearly, there are some geologic factors contributing to the scatter. To explore this further, we separated the 50 stations into five terrains or categories (ratio value vs. terrain plot in Figure 2.6). The first category or terrain (red triangles) represent stations within the Basin and Range terrain. The green circles, cyan diamonds, and magenta squares represent the Peninsular Ranges, the Sierra Nevada terrain, and the Pacific coast, respectively (see also Fig. 2.1). Stations further than 750 km are plotted as blue hexagons.

Figure 2.6 A map of the western U.S. showing station locations that correspond to specific spectral ratio values of the ratio Lg (4-6)/(2-4). In the upper right are two plots of the ratio values. One plot shows the log of the ratio values versus distance. The symbols equate to the terrain of the corresponding station as shown in Figure 1 but now with the addition of shades of grey: dark triangles = Basin and Range; light circles = Peninsular Ranges of southern California; light grey diamonds = Sierra Nevada; medium grey squares= Pacific Coastal region on the other side of the Great Valley from NTS; white hexagons = stations located greater than 750 km from NTS. The horizontal lines represent the mean and one (±) standard deviation of the mean. The length of these lines span a distance range that represents the stations used to determine the average. Stations outside this distance range are plotted for reference but were not used to calculate the average. On the map, values greater than one standard deviation are shown as white triangles. Values greater than the mean but less than one standard deviation are shown as white circles. Values less than the mean but greater than one standard deviation (-) are shown as light black circles. Values less than one standard deviation (-) are shown as black triangles. The rings approximate the distance from NPE in kilometers. The geologic terrains are outlined in white. The second plot in the upper right is a terrain plot showing the ratio values relative to terrain so that the effect of terrain may be more easily evaluated. Notice that the ratio values of the stations in the Basin and Range are distinctly lower than the other stations

Lg(4 - 6) / Lg(2 - 4)

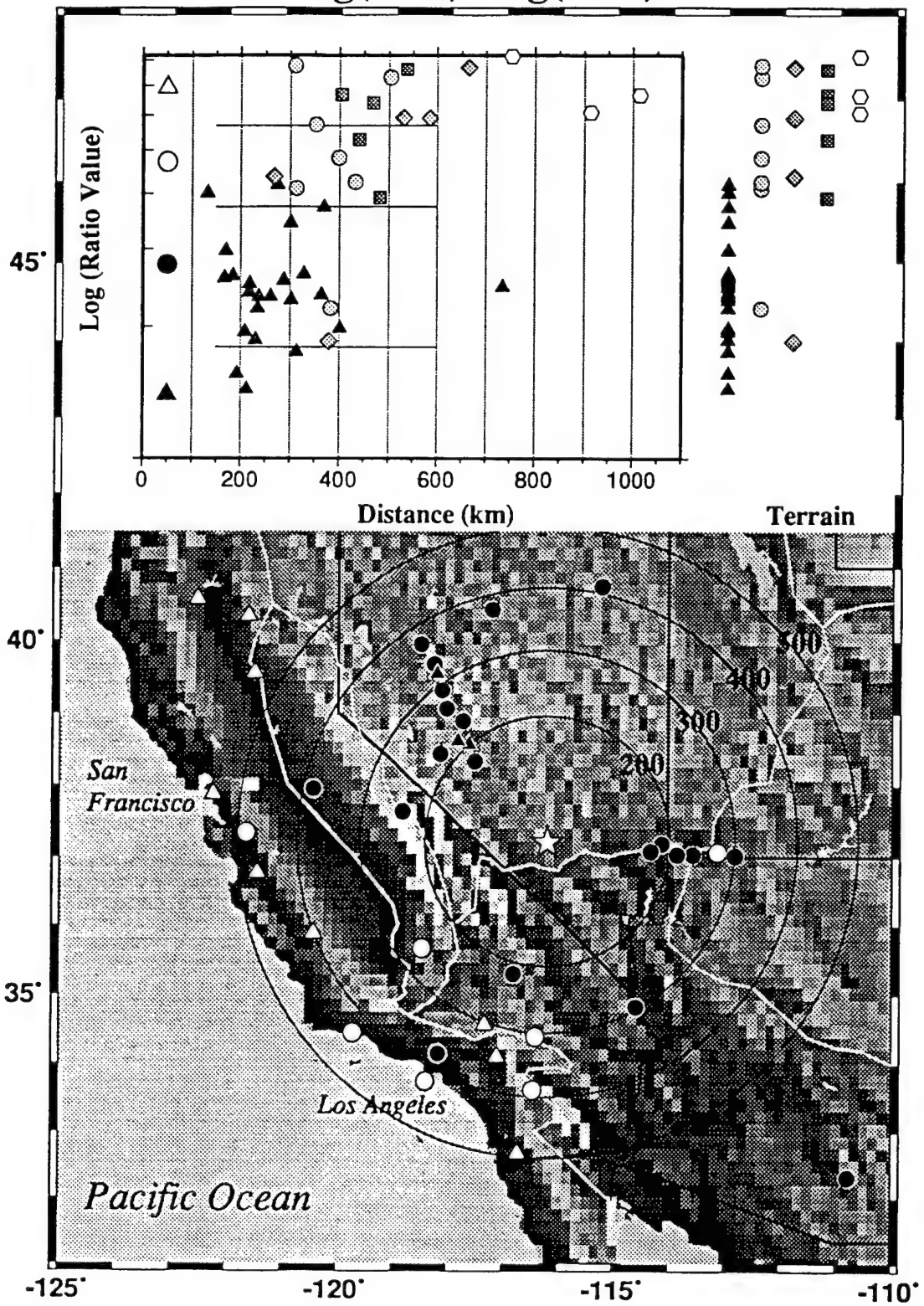
Log (Ratio Value)
0
200
400
600
800
1000
Distance (km)
Terrain
45°
40°
35°
-125°
-120°
-115°
-110°
100
200
300
400
500
San Francisco
Los Angeles
Pacific Ocean

We observe a separation of the ratio values based on terrain. Ratio values for stations within the Basin and Range cluster at a lower value than for stations outside of the Basin and Range.

Pn/Pn

Pn is also frequently used as a discriminant within some portion of the 1 - 10 Hz frequency band. As mentioned earlier, Pn amplitude can be markedly affected by Moho topography causing focusing and defocusing of energy. To quantify this for all stations, we compared the amplitude of Pn (1- 6 Hz) to the decay constant of $\Delta^{-(1.29 + 0.05 f)}$. The plot in Figure 2.7 shows the proportionality constant relating the observed Pn amplitude and expected Pn amplitude according to the decay constant as a function of distance. The horizontal lines in the plot represent the average and one standard deviation of the mean of the values. Shown on the map (Fig. 2.7) are the stations and their corresponding proportionality values relative to the mean. Therefore, value greater than the mean represents amplified Pn energy and values less than the mean represent diminished Pn energy. For example, the amplified Pn energy at station 5 on the UA line (Fig. 2.2) and BRH5 on the northwest line (Fig. 2.3) can be seen (red triangles, Fig. 2.7). Clearly, this factor alone will contribute to complexities in using Pn as a discriminant. Thus, we compared in Figure 2.8 the spectral ratio Pn (2-4)/(4-6) as a function of azimuth. The ratio values span slightly more than one order of magnitude. Along the portable profiles, Pn is clearly affected by azimuth; the UA line has higher than average ratio values (red in Fig. 2.8) and the Northwest line has lower than average values (blue in Fig. 2.8). Since these seismic profiles had variable Pn amplifications (Fig. 2.7), the Pn path must have an effect. In other words, Pn is influenced by Moho structure. Furthermore, for all the stations, there is no separation in the ratio values based on terrain; all the terrain values plot within the scatter of the Basin and Range values. Thus, the contribution of Pn energy is a function

Figure 2.7 A plot of the proportionality constant between the Pn energy observed and that expected from the determined decay constant vs. distance. The horizontal lines represent the mean and one (±) standard deviation of the mean. On the map, values greater than one standard deviation are shown as white triangles. Values greater than the mean but less than one standard deviation are shown as white circles. Values less than the mean but greater than one standard deviation (-) are shown as black circles. Values less than one standard deviation (-) are shown as black triangles. Thus, the high values (white triangles) represent amplified Pn energy and the low values (black triangles) represent diminished Pn energy. The rings approximate the distance from NPE in kilometers.

Pn Energy off Moho

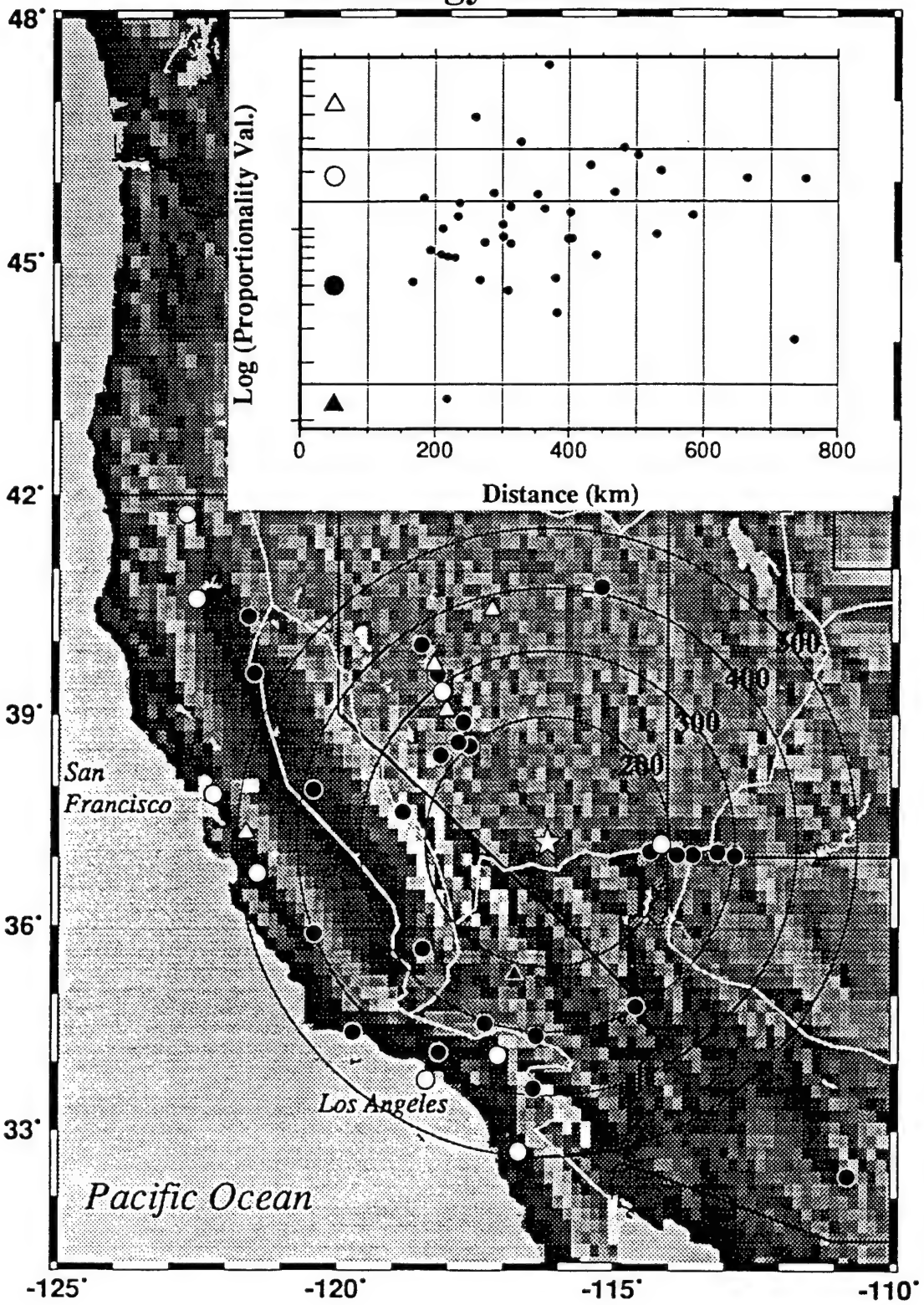

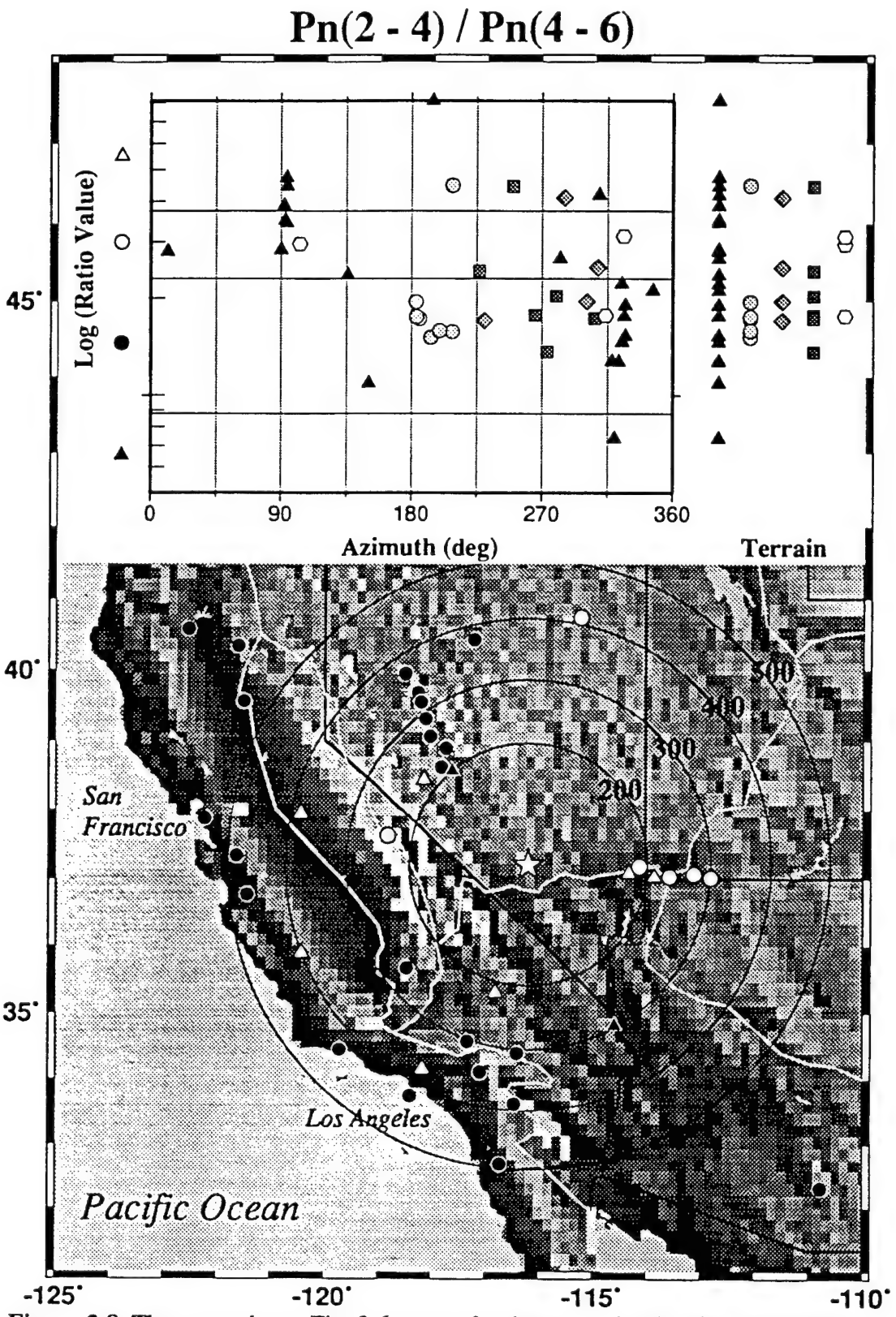

Figure 2.8 The same plot as Fig. 2.6 except for the spectral ratio of Pn(2-4)/(4-6) is plotted as a function of azimuth.

of Moho structure, which correlates with azimuth, and though not observed in the ratio values, is associated with geologic terrain.

Pn/Lg

As seen in Figure 2.9, the cross-spectral ratio Pn (1-2) / Lg (2-4) values are plotted as a function of distance. There is a reasonable separation in the ratio values between those stations inside the Basin and Range compared to other terrains (Fig. 2.9). However, there is also more scatter in these values compared to the first two examples (Figs. 2.6 and 2.8) with this particular phase ratio spanning two orders of magnitude. Thus, when comparing the ratio value to a preexisting earthquake and explosion population, the station used would markedly influence the amount of separation observed. On average, stations located outside the Basin and Range tend to have higher ratio values than those stations located within the Basin and Range.

Hunter's Trophy Phase Comparison

The source spectrum of NPE is approximately twice that for a nuclear explosion of similar yield and detonated in similar material (Goldstein and Jarpe, 1994; Denny et al., 1996). This occurs due to the fact that chemical explosions are much more efficient with coupling energy into the ground (Denny et al., 1996). However, in a discrimination setting, yields will not be reported and must be determined seismically or via other instrumentation. Thus, the scaled source spectra of NPE to a similar nuclear explosion were analyzed and found to be virtually identical (Denny et al., 1996) especially at higher frequencies (Goldstein and Jarpe, 1994). At local and regional distances, the waveform data between NPE and similar nuclear explosions is remarkably similar (Smith, 1994; Walter et al., 1994).

On September 18, 1992, almost one year to the day earlier then NPE, a low yield ($m_b \approx$ 4.4) nuclear device named HUNTER'S TROPHY was detonated in N-tunnel at NTS. The

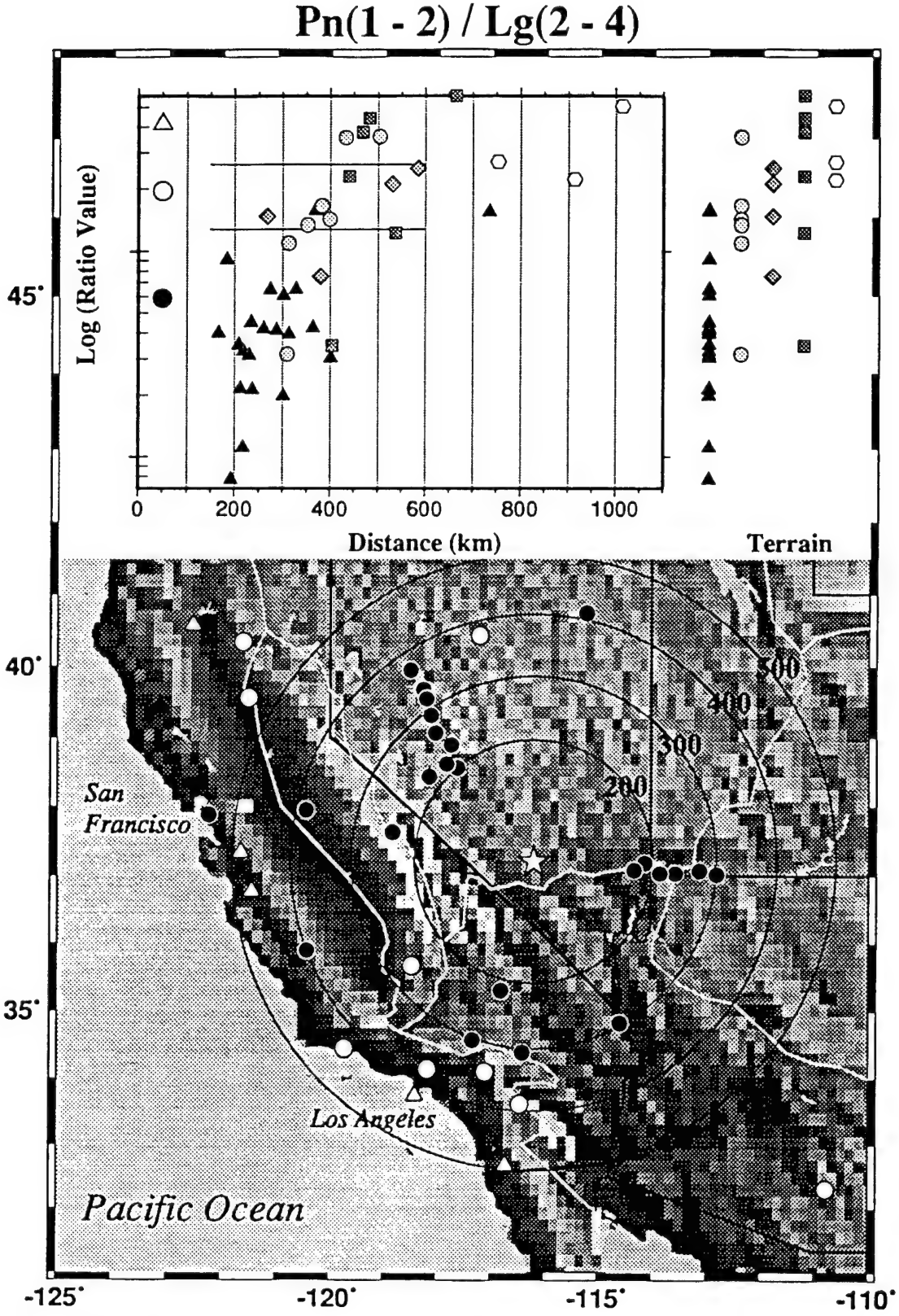

Figure 2.9 The same plot as Fig. 2.6 except for the cross-spectral ratio of Pn (1-2)/Lg(2-4).

location was only 500 meters away from the NPE detonation. Since the locations and magnitudes of HUNTER'S TROPHY and NPE are virtually the same, these two events are ideal for comparison between nuclear explosion and chemical explosion waveform signatures. Fourteen permanent stations recorded these two explosions; Pn at nine stations and Pg at five stations. The Pn (Fig. 2.10) and Pg (Fig. 2.11) broadband waveforms not only show remarkable similarity in terms of shape but amplitude as well. The ratio value indicated in each box is the ratio of the first swing of P from HUNTER'S TROPHY (HT) to NPE. The Pn mean ratio for the 9 stations is 0.99, indicating the amplitude for the two events is virtually the same. Similarly, the Pg mean ratio value is 1.45. There appears to be no correlation of ratio value with distance or azimuth. Furthermore, Walter et al. (1995) performed a thorough analysis of short-period phase and spectral ratio discriminants for 130 nuclear explosions, NPE, and 50 earthquakes that occurred at NTS and were recorded on two LLNL stations. Regardless of the discriminant, NPE always plotted within the explosion populations. Thus, because the seismic difference between a single-hole chemical explosion and similar yield nuclear explosion is small, chemical explosions could be used to seismically calibrate other regions of the world.

DISCUSSION

With the need to monitor small events, discrimination has recently focused on regional techniques. However, smaller earthquakes have shorter (more explosion-like) source durations. Thus, regional discriminants usually focus on P and S energy at higher frequencies where fortunately, they are the most effective. Regional spectral discrimination has had a long history (Bakun and Johnson, 1970; Bennett and Murphy, 1986; Taylor et al., 1989). Taylor et al. (1988) explored the spectral ratios ((1-2)/(6-8)) of Pg, Pn, and Lg for explosions and western U.S. earthquakes. Walter et al. (1995) studyed the same spectral ratios, as well as the phase ratio Pn/Lg. They observed a good separation of the

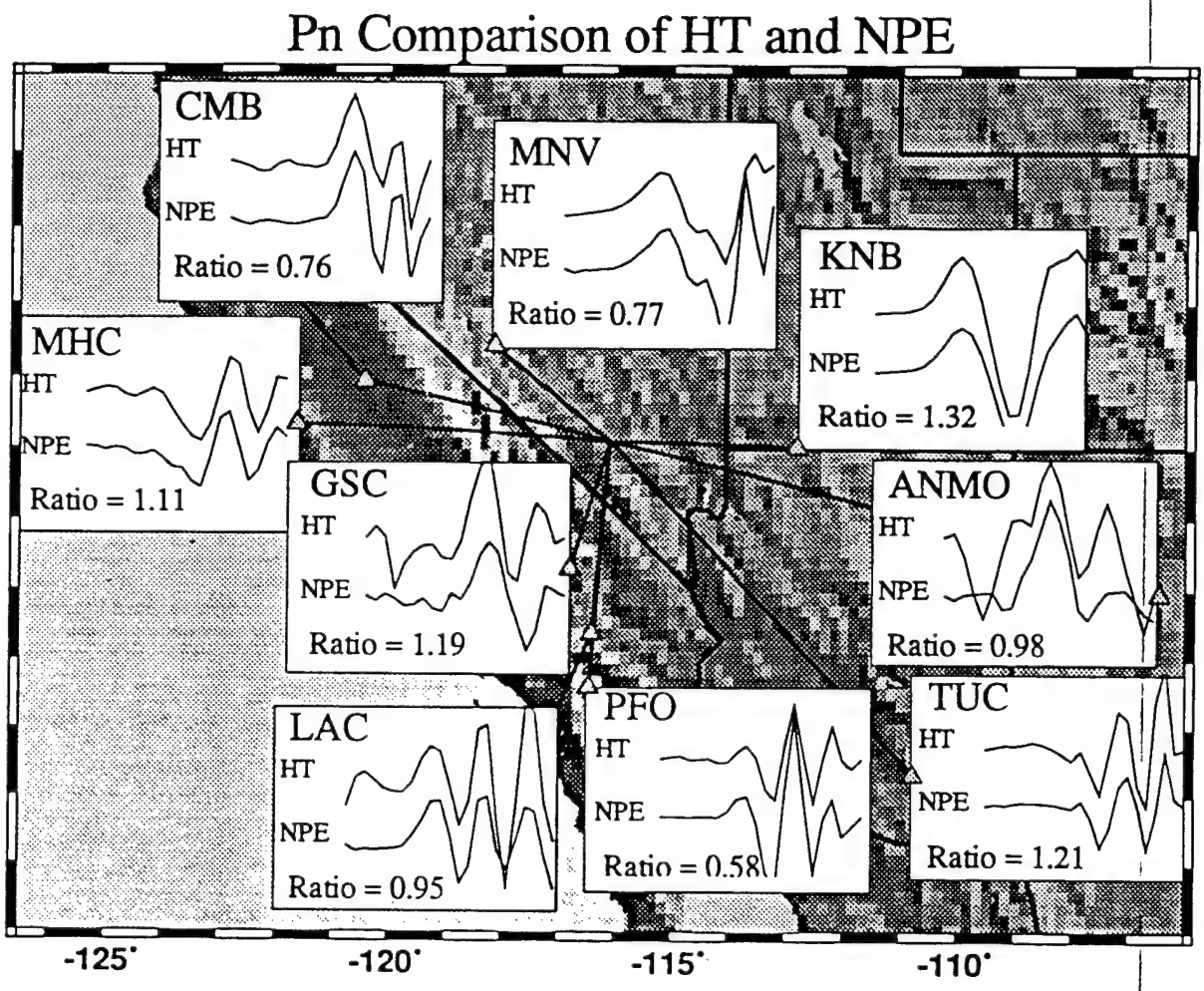

Figure 2.10 A map showing the locations of the broadband stations that recorded Pn from both HUNTER'S TROPHY (HT) and NPE. The white boxes show the Pn waveform generated by each explosion. The ratio value represents the ratio between the amplitude of the first swing of Pn from HT to the amplitude of the first swing of Pn from NPE.

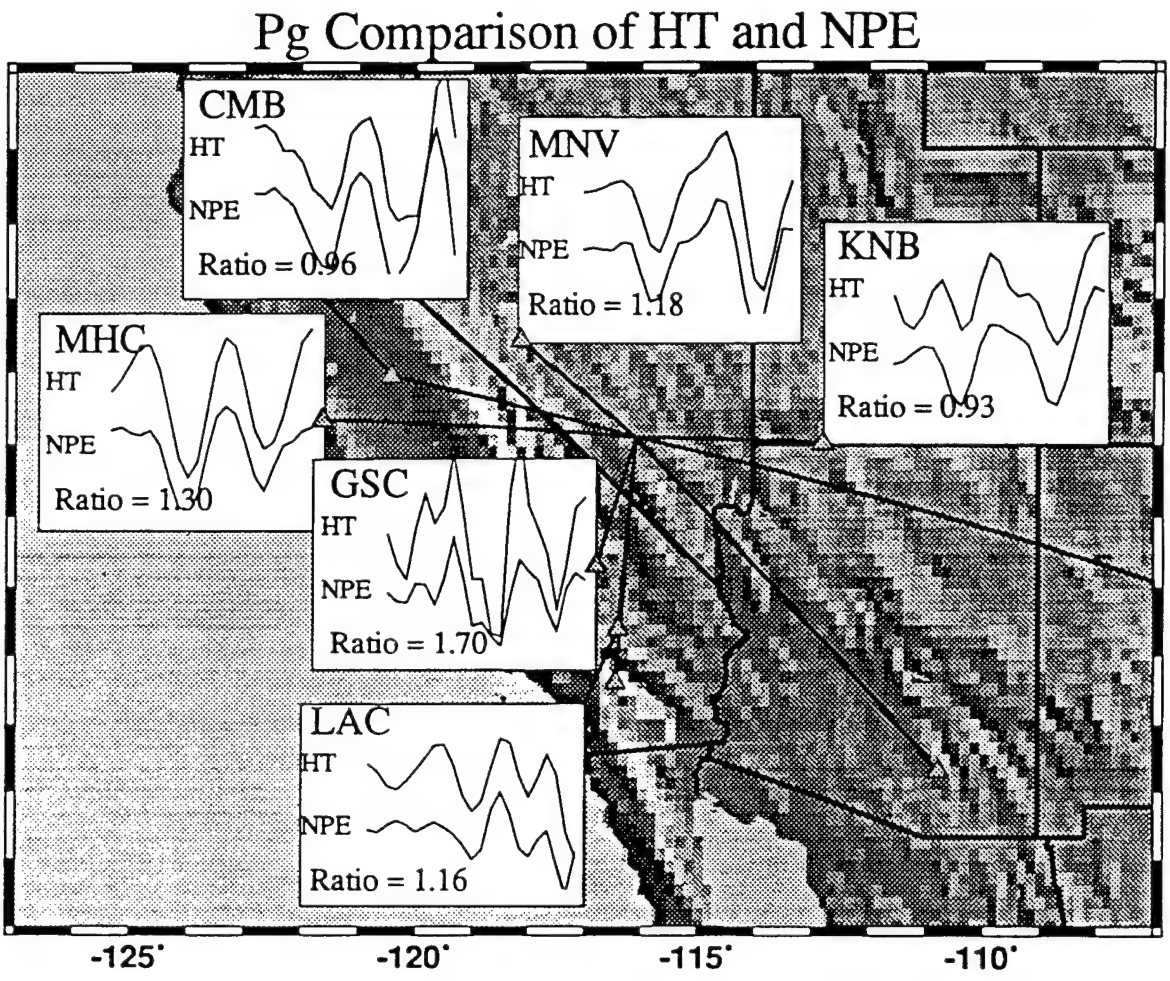

Figure 2.11 A map showing the locations of the broadband stations that recorded Pg from both HUNTER'S TROPHY (HT) and NPE. The white boxes show the Pg waveform generated by each explosion. The ratio value represents the ratio between the amplitude of the first swing of Pg from HT to the amplitude of the first swing of Pg from NPE.

explosion and earthquake populations located in and near NTS. However, the power of these techniques lies within the path calibration. In these cases, the only stations used to evaluate the discriminants were the four LLNL stations located around NTS (approximately 220 km to 400 km distance). As stated earlier, this is because these are the only stations in operation long enough to provide a sufficient catalog. Thus, the major difference in the waveforms of Walter et al. (1995) is the result of source and not the result of path and hence, the effectiveness of each discriminant can be evaluated. Taylor et al. (1988) applied a simple first order distance correction to their data set. However, to monitor a CTBT, regional discriminants will be applied to data recorded at regional distances. Thus, path calibration must be derived from earthquakes if the area is seismically active. If it is also to be compared to a population of events recorded elsewhere, such as NTS, it will be necessary to remove path effects based on the geologic terrain traversed.

A promising regional discriminant, Pn/Lg, incorporates the higher frequencies of P and S energy. However, we observe variations in the P and S energy as a function of azimuth and distance. As seen in Figure 2.6, the lower ratio values of Lg (4-6)/(2-4) (red triangles on the ratio value plot) correlate with stations located in the Basin and Range. For stations located outside the Basin and Range, the ratio values are considerably higher (green circles, cyan diamonds, magenta squares, and blue hexagons). Is this truly a terrain effect? Because NTS is located within the Basin and Range, stations located in other terrains are farther away. Thus, it is possible we are not observing a terrain effect but a distance effect, implying that we may not have effectively removed geometrical spreading. However, as seen in Figure 2.6, there is clear separation between stations within the same distance range ($\leq$ 400 km) based on terrain. Furthermore, station TUC in Tucson, Arizona, is located $\approx$730 km from NTS. This distance is nearly double that of the next farthest station from NTS yet still located in the Basin and Range. The ratio value for TUC plots in the center of

the range of Basin and Range values. Thus, it appears Lg is affected by terrain, not azimuth or distance.

The phase Pn is markedly affected by azimuth. The two portable profiles, both of which are primarily located within the Basin and Range (stations 1-3 from the UA profile are in the Colorado Plateau), show consistently different values for the ratio Pn (2-4)/(4-6); the UA profile has higher ratio values than the Northwest profile (Fig. 2.8). The UA profile in Figure 2.12 was simplified from Zandt et al. (1995), and the Northwest profile was created from the simplified structure discussed earlier. Pn energy samples deeper into the mantle for the UA profile than for the Northwest profile. Thus, it is possible that the higher frequencies are attenuated more under the Colorado Plateau resulting in the higher ratio values shown in Figure 2.8. Furthermore, with the exception of the UA profile, all stations with a ratio value above the average (red triangles and red circles) appear to be randomly distributed. In other words, the high ratio values have no correlation with distance, azimuth, or terrain. However, without exception, these stations all correspond to a diminished Pn arrival shown as blue circles or triangles in Figure 2.7. In other words, a station with an above average Pn (2-4)/(4-6) value has a below average Pn proportionality constant, implying that at these stations, Pn (4-6) decreased more than Pn (2-4) relative to other stations. Thus, where Pn is diminished, the longer periods are attenuated less.

In summary, Pn is a difficult phase. Its energy is not directly effected by regional crustal velocities associated with geologic terrain as seen in Figure 2.8, where the ratio values all plot within the spread of the Basin and Range. However, it can be effected by geologic terrain in terms of Moho depth and structure. We note that the focusing and defocusing of Pn energy shown in Figure 2.7 is only applicable for sources at NTS. In other words, these same stations may not experience amplification at different back

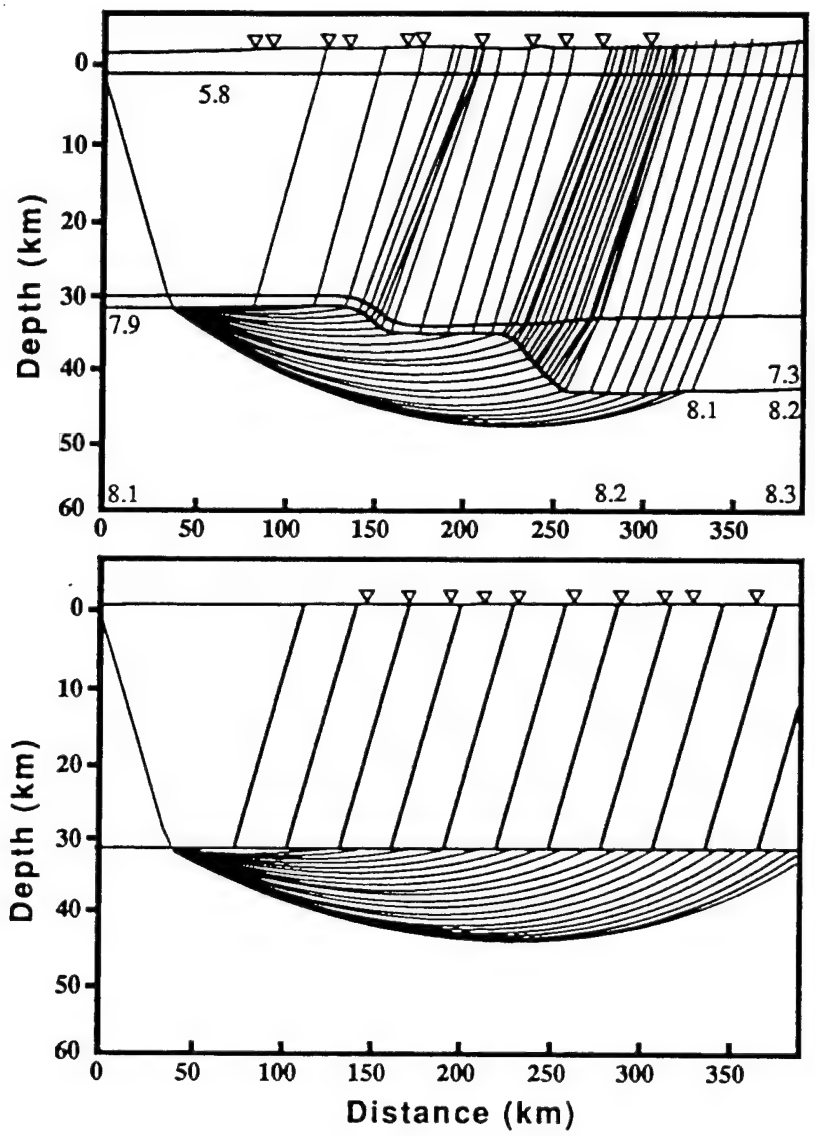

Figure 2.12 Pn ray path from NTS along the UA line from Zandt et al. (1995) (top). Pn ray paths from NTS along the Northwest profile using a simplified structure from McCormack et al. (1994) (bottom). Notice the Pn energy samples deeper into the mantle along the UA line.

azimuths since the Moho path is different. Therefore, a single station cannot be tagged solely as amplified or diminished; it is also a function of back azimuth.

The different frequency band measurements of the phase ratio Pn/Lg do not readily produce azimuthal or terrain station patterns. However, this is to be expected since the ratio Pn/Lg is a product of both a phase influenced by geologic terrain (Lg) and a phase influenced by Moho structure and azimuth (Pn). Thus, these factors must be accounted for when interpreting the ratio value of each station in, for example, Figure 2.9. There is a reasonable separation of Pn (1-2) / Lg (2-4) values based on terrain as seen in the upper right of Figure 2.9. Stations located within the Basin and Range have a smaller ratio value than stations located within the other terrains. This phenomena is the effect of the Lg contribution. The Pn contribution is more difficult to analyze. Depending on which frequency window of Pn is used, the Pn contribution tends to add scatter to the ratio values. In other words, the ratio values of the terrains tend to be less clustered and exhibit more overlap (Fig. 2.9).

What are the implications of using regional discriminants? If NPE was a suspect event that was recorded by a few stations, then the ratio value at those stations would be compared either to other known explosions/earthquakes recorded at those same stations and preferably along the same path (in other words, calibrated paths) or to an earthquake/explosion dataset generated with other stations from some other region of the world. This comparison would be used to determine if the event was an explosion or an earthquake. Preferably, and realistically, the earthquake catalog for the seismic stations that recorded the suspect event would contain earthquakes from approximately the same region with which to make direct comparisons and path evaluations. However, as demonstrated in this paper, the uncertainty would be large without an extremely thorough data set. Nonetheless, the earthquake/explosion dataset from NTS is the best in the world and

should be utilized. Thus, cross-comparisons between a known source-station (NTS and station KNB, for example) and the suspect source and station located in a different region of the world is inevitable. To avoid potential mis-identifications, path effects, site effects, and source media from both datasets (NTS and suspect) should all be considered so that comparisons truly evaluate source differences.

CONCLUSIONS

Regional discriminants are necessary to monitor low yield explosions. However, regional phases can be very complicated due to path effects, thus affecting transportability of discriminant techniques from area to area. We find values of the discriminant Pn/Lg to behave according to both the geologic terrain and the large (gross orientation) and small (topography) scale Moho structure of the path traversed. Specifically, Pn (1-2) / Lg (2-4) has values nearly one order of magnitude less for stations located within the Basin and Range then stations located outside the Basin and Range. The spread of the Lg/Lg and Pn/Pn values is within one order of magnitude while the Pn(1-2) / Lg(2-4) values cover 1.8 orders of magnitude. The increased scatter in the Pn(1-2) / Lg(2-4) values within terrains, as well as the increased overlap between terrains, is due to the Pn contribution. Nonetheless, the Pn/Lg values still separate according to terrain due to the Lg contribution. If the luxury of a calibrated path does not exist, then these path phenomena must be accounted for when evaluating a suspect event.

ACKNOWLEDGEMENTS

We wish to thank George Zandt, Steve Myers, Jennifer Swenson, Guangwei Fan, and Richard Brazier for helping with the operation of the U of A profile. Bill Walter, Peter Goldstein, George Zandt, and an anonymous reviewer provided constructive comments. The instrumentation was provided by the PASSCAL data center. Funding for this analysis

was provided by AFOSR under ASSERT grant F49620-93-1-0498. SASO contribution #83.

CHAPTER 3

THE SIX RECENT FRENCH NUCLEAR EXPLOSIONS: A RELATIVE DETERMINATION OF LOCATION, MAGNITUDE, AND YIELD USING OPEN BROADBAND STATIONS

INTRODUCTION

On September 24, 1996, President Clinton signed the Comprehensive Test Ban Treaty (CTBT) which will prohibit the testing of nuclear weapons. Enforcement of a CTBT requires monitoring the entire planet for potential evaders; however, this is not a trivial task. To address this, the Group of Scientific Experts Third Technical Test (GSETT-3) began full scale operations in January of 1995 at the prototype International Data Center (IDC) at the Advanced Research Projects Agency's (ARPA) Center for Monitoring Research in Arlington, Virginia. The purpose of this global seismological experiment was to develop an international system that could evolve into the International Seismic Monitoring System for the CTBT. Thus, it would become an international data center geared towards global monitoring.

Over 90% of the stations reporting to the GSETT-3 are part of the Incorporated Research Institutions for Seismology (IRIS) Global Seismographic Network (GSN) or are part of other "open" networks which are accessible to the academic community in near real time. A complimentary experiment to GSETT-3 is the "routine" processing of seismic waveforms to determine, for example, location and magnitude (see http://www.cdidc.org/ on the world wide web). The majority of these waveforms are available in near real time through the IRIS Data Management Center. Presently, groups like the Harvard Centroid Moment Tensor project utilize these data to provide rapid earthquake source parameters.

Similar projects can be designated to "monitor" specific regions of the world or seismic phenomena other than earthquakes.

After a four year moratorium, France resumed their nuclear testing program in the Pacific by conducting six tests during a five month period that began in September of 1995. Newly elected president Chirac stated that France needed to test the reliability of their nuclear stockpile in a one-time-only series of tests. Furthermore, he also stated they were in full support of a CTBT. Other than China's active testing program, there had been no nuclear tests since September of 1992 when the United States conducted its last test codenamed DIVIDER (m_b = 4.4, September 23, 1992). Thus, the French explosions provided a unique opportunity to evaluate the waveform products from open stations and automated retrieval mechanisms such as the IRIS Spyder™ system.

DATA

We obtained broadband data from the affiliated networks of IRIS (GSN, TERRAScope, GTSN) using the IRIS Spyder™ and X-retrieve interfaces. We also retrieved data for seven stations from the Berkeley Digital Seismic Network (BDSN) world wide web homepage. A total of 17 teleseismic stations were used to determine magnitudes (m_b), and a total of 24 teleseismic stations were used to determine hypocenters (Fig. 3.1). We employed a simple technique to determine the relative magnitudes (m_b) and used the Joint Hypocenter Determination (JHD) software of Dewey (1971, 1983) to determine relative hypocenters. All waveform data were from open stations and can be retrieved in near real time by anyone with access to the internet. Furthermore, this open data can easily be used by anyone to determine locations and magnitudes.

MAGNITUDE, YIELD, AND LOCATION

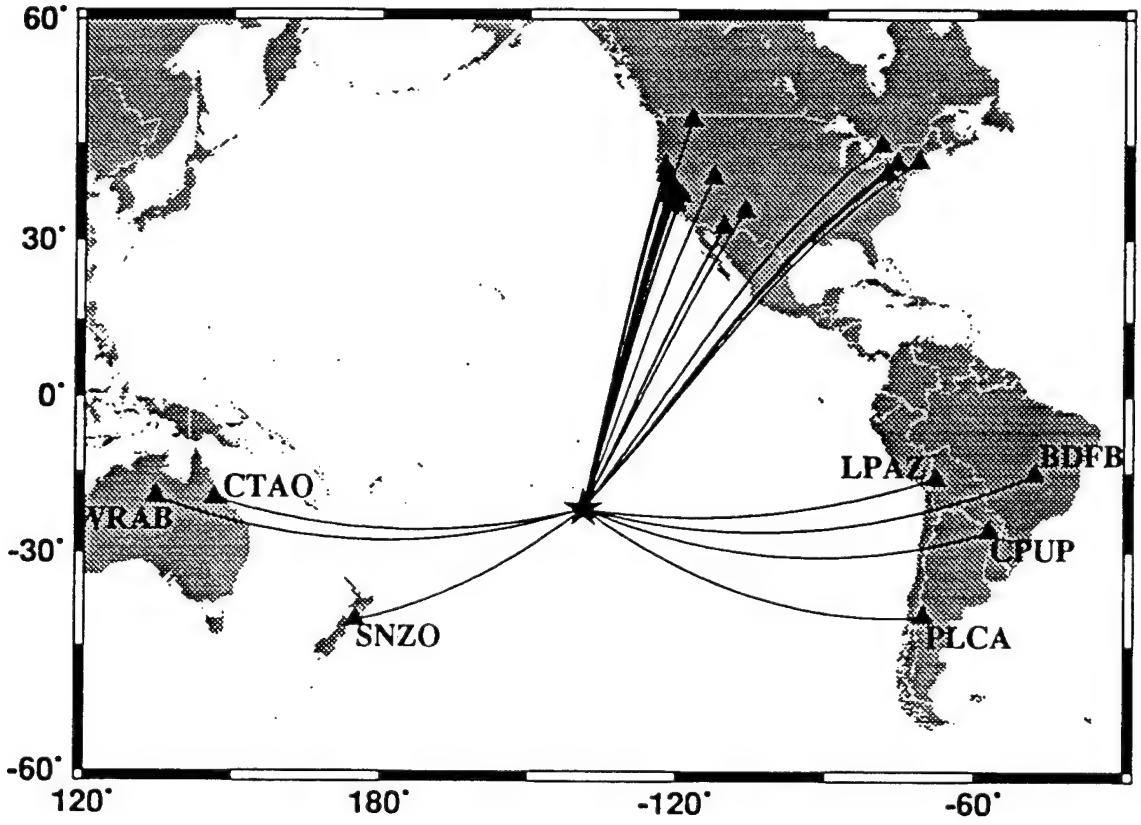

Figure 3.1 A map showing the great circle paths from the French testing site (star) to all the stations used in this study.

Both the determination of magnitudes and locations are relative to a reference or "master" event. We chose the explosion on October 1, 1995, as the master event, because it was recorded by the most stations, which implied it would have the best "location." Further, it most likely had the largest magnitude and thus, yield. The seismically determined coordinates reported by the IDC located this explosion directly on Fangataufa, a Pacific seamount in French Polynesia that had been used in other French nuclear tests. A comparison of waveforms (1 Hz) recorded at station CMB from the six explosions is shown in Figure 3.2. The y-axis scale is the same for all six records; the variation in amplitude is a function of magnitude (yield). Although there is remarkable similarity among the P-wave arrivals, there are slight differences that we attribute to variations in source depth.

Body wave magnitude is based on the the actual ground motion amplitude (A) of the first few cycles of the P wave corresponding to a specific period (T). The amplitude and period are logarithmically related to m_b by

$$m_b = (\log A/T) + Q(h, \Delta) \quad (1)$$

where $Q(h, \Delta)$ is a correction for distance and depth. However, we are interested in the change in magnitude (ΔM) from a master event. Therefore, if we assume the same hypocentral location, at any particular station

$$\Delta M = \log (A_m/T_m) - \log (A/T) \quad (2)$$

where the subscript "m" signifies the master event. We limited the frequency content of the signal to 1 Hz. Thus, $T_m = T$, and equation (2) reduces to

$$\Delta M = \log (A_m / A). \quad (3)$$

We used 17 stations that all recorded the master event on October 1, 1995, and at least three of the other explosions. The November explosion was recorded by the fewest number of stations, because it was one of the smallest in magnitude. As reported by IRIS, the October

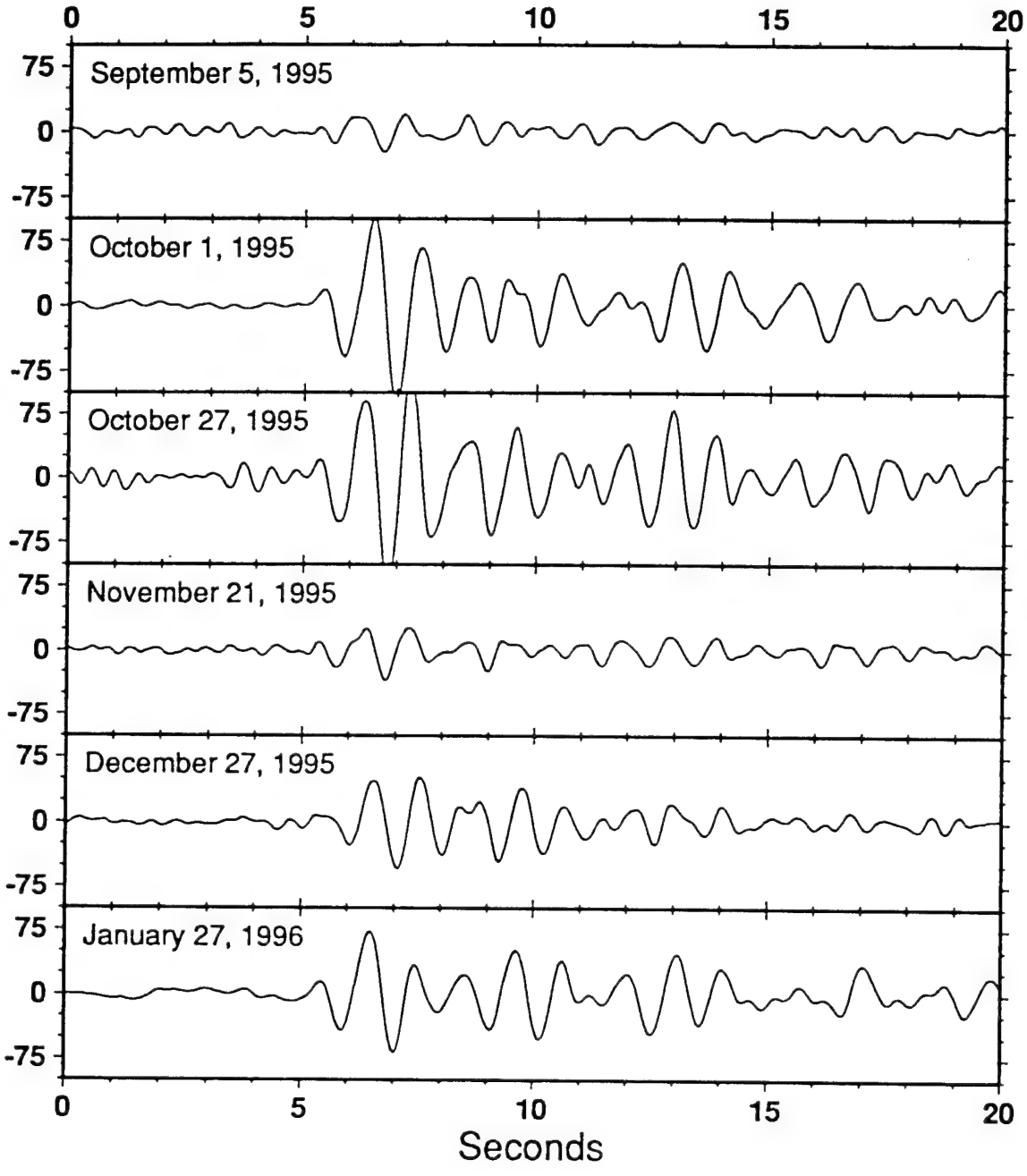

Figure 3.2 A comparison of P-waveforms from the six explosions recorded at station CMB in California. All traces have been high passed filtered at 1 Hz and are plotted at the same y-axis scale. Thus, variation in amplitude is a function of magnitude (yield). of the first swing of Pn from HT to the amplitude of the first swing of Pn from NPE.

1, 1995, master event had a magnitude of 5.5. We determined the mean and one standard deviation of the change in magnitude determined at all stations for each event (Table 3.1).

TABLE 3.1. The explosion epicenter, origin time, magnitude, and estimated yield

Date	Julian Day	Origin Time	Latitude (deg)	Longitude (deg)	Magnitude (m_b)	Yield (kt)
Sep 5	(248)	21:29:59.61	21.894 S	138.760 W	4.78±.2	≈ 3
Oct 1*	(274)	23:29:59.40	22.25 S	138.76 W	5.5	≈ 25
Oct 27	(300)	21:59:59.72	21.883 S	138.994 W	5.41±.1	≈ 19
Nov 21	(325)	21:29:59.80	21.917 S	138.952 W	4.82±.2	≈ 3
Dec 27	(361)	21:29:59.91	21.840 S	138.890 W	5.00±.2	≈ 5
Jan 27	(027)	21:29:59.37	22.270 S	138.750 W	5.37±.1	≈ 17

*October 1 is the master event

Seismically determined yields can be very difficult to estimate. Although the determination of magnitude/yield relationships is straightforward given the magnitude of explosions of known yield, the number of reported yields is small. Furthermore, most of these reported yields are for explosions conducted at the Nevada Test Site. It has been established that yields determined seismically are a function of the source medium and the travel path between source and receiver. The NTS magnitude/yield relationships can be off by as much as a factor of 2 when applied to other source regions (Douglas and Marshall, 1996). Generally, the source media can be divided into two end-member groups. Good coupling, which is usually obtained in hard or water saturated rocks, and poor coupling, which usually occurs in dry or porous rocks. Assuming the islands to be water saturated basalts, we used the following relationship derived from media associated with good coupling

$$m_b = 4.45 + 0.75 \log (Y) \qquad (4)$$

where m_b is the body wave magnitude and Y is the yield (Douglas and Marshall, 1996). From this, we determine the yield of the October 1, 1995, reference event (m_b = 5.5) to be 25 kt. The remaining yields are given in Table 3.1.

The yield relation in (4) should be considered a minimum estimate for two reasons. First, the coupling for this source region may be lower than the worldwide average. Secondly, the magnitude reported by IRIS for the October 1, 1995, master event may be low. If either of these circumstances are valid, the yields reported in Table 3.1 could increase by a factor of two.

We used the Joint Hypocenter Determination (JHD) method to determine explosion locations (Dewey, 1971, 1983). This method simultaneously calculates all the hypocenters relative to the October 1, 1995, reference event. Thus, the independent effects of travel time anomalies introduced by the different travel paths to the recording stations will be statistically minimized, resulting in more accurate locations relative to the October 1, 1995, reference event. We only used P-wave arrival times, because the onset time for S waves from explosions are less clear. A total of 24 stations located at teleseismic distances (<100°) were used. Sixteen of the stations recorded at least 4 of the explosions, while the remaining 8 stations recorded an average of two explosions. The epicentral coordinates and origin times are given in Table 3.1. The epicenter and error ellipses for the explosions are shown in Figure 3.3. All French nuclear tests in the Pacific must occur on seamounts if they are to be underground and contained. Thus, the locations should correlate with these islands.

DISCUSSION

France has had an active nuclear testing program; only the United States and the former Soviet Union have conducted more tests. France conducted the last of approximately 15 nuclear tests in Algeria in early 1966. By late 1966, they had conducted their first test on the Pacific island of Mururoa in the Tuamoto Archipelago, a portion of French Polynesia

The Recent French Nuclear Explosion Locations

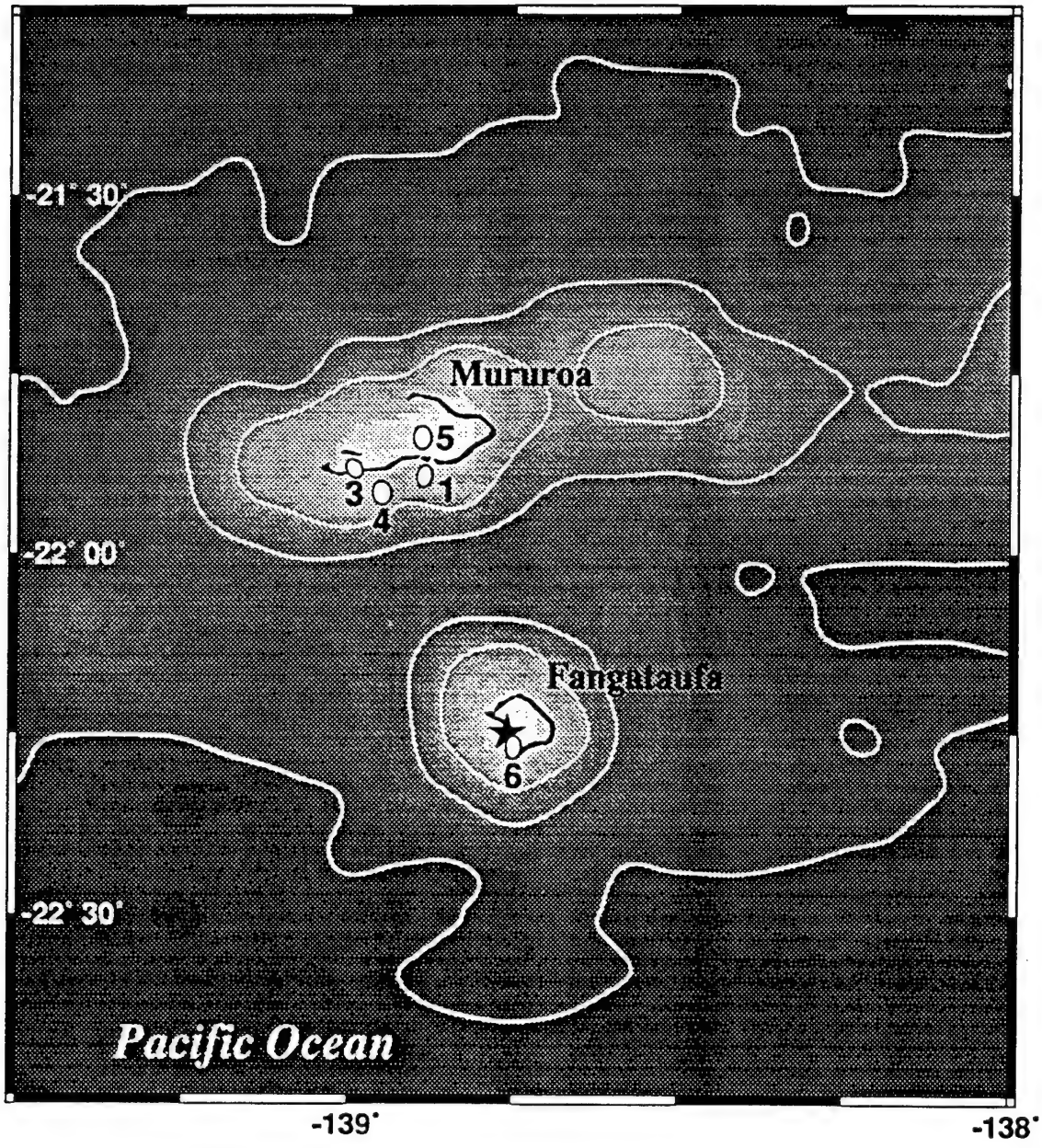

Figure 3.3 A map of the French testing site in the Pacific. The contour lines represent the -2000 m, -3000 m, and -4000 m bathymetric contours. The location of the master event (October 1, 1995) is shown by a black star. The relative locations of the remaining 5 explosions are indicated by their error ellipses and numbered chronologically. Recall that Mururoa and Fangataufa are atolls. Therefore, the only "dry land" is a ring of coral as indicated in black. The interior portion of the "island" is living coral under shallow water.

(Fig. 3.4). The French have conducted at least 110 tests on Mururoa, with magnitudes ranging from 4.0 to 5.9 (Lawson, 1994). They have also conducted approximately 8 tests on the neighboring island of Fangataufa (Lawson, 1994) including the first underground explosion at their Pacific test site on June 5, 1975 (Dahlman and Israelson, 1977). Up until that point, many of the early French Polynesia tests (≈35) were above ground. Mururoa and Fangataufa are atolls, seamounts ringed in coral that constantly grow upwards, striving for the sunlight and warmer water necessary for their survival, as the extinct volcano beneath them slowly sinks with the aging seafloor.

An island in the middle of the ocean is a "worse case scenario" for seismic monitoring. Almost without exception there are no seismic stations within regional (< 1500 km) distances. Stations that are less than 1500 km away are usually located on an island themselves and are "noisy." High seismic noise levels are created by oceanic waves striking the island. The high noise levels reduce the detection capability. Thus, waveforms from mid-oceanic explosions are usually only well recorded at teleseismic distances.

Using teleseismic data from open seismic stations we determined that four of the explosions occurred on the island of Mururoa and the remaining two explosions occurred on Fangataufa. The global array of open seismic stations allows monitoring down to small magnitudes; thus, relative magnitude and location determination is not limited to explosions recorded at selective stations. Anyone with access to the internet and moderate computing facilities can determine relative magnitudes and locations for earthquakes as well. Via the internet we were able to obtain a photograph (Fig. 3.4) of Mururoa taken by the six person crew of the space shuttle Endeavor just 23 days after the last French nuclear test (December 27) on that same seamount (http://images.jsc.nasa.gov/html/earth.htm).

The rapidly growing internet provides a phenomenal amount of information that is easily and quickly obtainable. In terms of seismic monitoring, the information era fosters

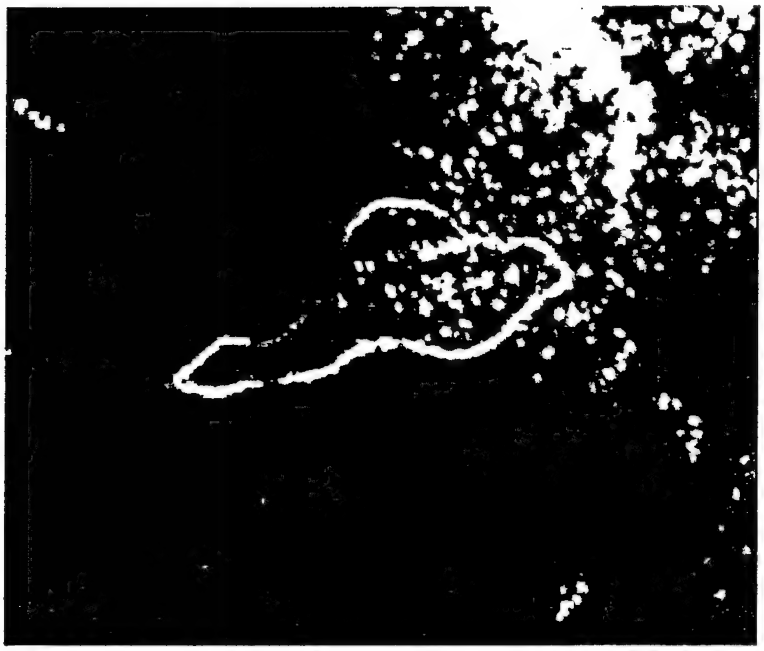

Figure 3.4 A photo of Mururoa taken by the crew of the space shuttle Endeavor during the 74th shuttle mission (STS-72). The photo was originally taken in color at an altitude of 164 nautical miles on January 19, 1996, 23 days after the last French test on that same seamount.

the concept of a "neighborhood watch," where seismic data is exchanged freely and efficiently. Open access combined with the routine global monitoring of the GSETT-3 experiment provides the backbone of a seismic system which is difficult to evade.

ACKNOWLEDGEMENTS

Thanks to Dr. Gregory E. van der Vink and John Ebel for their thorough reviews. Funded by AFOSR ASSERT grant #F49620-93-1-0498. Data provided by the IRIS DMC, a NSF funded facility, and BDSN.

REFERENCES CITED

Bakun, W.H. and L.R. Johnson (1970). Short period spectral discriminants for explosions, *Geophys. J. R. Astr. Soc,* **22**, 139-152.

Beck, S., P. Silver, T. Wallace, and D. James (1995). Directivity Analysis of the Deep Bolivia Earthquake of June 9, 1994, *Geophys. Res. Lett.*, **22**,

Beghoul, N., M. Barazangi, and B.L. Isacks (1993). Lithospheric structure of Tibet and Western North America: Mechanism of uplift and a comparative study, *J. Geophys. Res.*, **98**, 1997 - 2016.

Bennett, T.J. and J.R. Murphy (1986). Analysis of seismic discrimination using regional data from western United States events, *Bull. Seism. Soc. Am.*, **76**, 1069-1086.

Beroza, G.C., and M.D. Zoback (1993). Mechanism diversity of the Loma Prieta aftershocks and the mechanics of main shock-aftershock interaction, *Science,* **259**, 210-213.

Chavez, D. and K.F. Priestley (1986). Measurement of frequency dependent Lg attenuation in the Great Basin, *Geophys. Res. Lett.*, **13**, 551-554.

Chun, K.Y., R.J. Kokoski, and G.F. West (1989). High-frequency Pn attenuation in the Canadian Shield, *Bull. Seism. Soc. Am.*, **79**, 1039-1053.

Dahlman, O., and Israelson, H. (1977). *Monitoring Underground Nuclear Explosions,* 440 pp., Elsevier Scientific Publishing Company.

Denny, M.D., P. Goldstein, K. Mayeda, and W. Walter (1996). Seismic results from DOE's Non-Proliferation Experiment: A comparison of chemical and nuclear explosions, in *Monitoring a Comprehensive Test Ban Treaty,* E.S. Husebye and A.M. Dainty eds., Kluwer Academic Publishers, Netherlands, 1996, 355-364.

Denny, M.D. (1994). Introduction and highlights, *Proceedings of the Symposium on The Non-Proliferation Experiment: Results and Implications for Test Ban Treaties,* April 19-21, 1994, M.D. Denny, ed., Rockville, MD, CONF-9404100, 1-1 - 1-17.

Denny, M.D. and J.J. Zucca (1994). Introduction: DOE Non-Proliferation Experiment, *Arms Control and Nonproliferation Technologies,* DOE/AN/ACNT-94A, First Qtr., 8-21.

Department of Energy, Office of Nonproliferation and National Security, *CTBT, Technical Issues Handbook,* UCRL-ID-117293

Dewy, J.W. (1971). Seismicity studies with the method of joint hypocenter determination. Ph.D. thesis, 164 pp., Univ. of Calif., Berkeley.

Dewy, J.W. (1983). Relocation of instrumentally recorded pre-1974 earthquakes in the South Carolina region, in Studies Related to the Charleston, South Carolina, Earthquake of 1886, edited by G.S. Gohn, *U.S. Geol. Surv. Prof. Pap.*, 1313, Q1-Q9.

Douglas, A., and Marshall, P.D. (1996). Seismic source size and yield for nuclear explosions, in *Monitoring a Comprehensive Test Ban Treaty,* edited by E.S Husebye and A.M. Dainty, p. 309 - 353, Kluwer Academic Publishers, Norwell, MA.

Frohlich, C. (1989). The nature of deep-focus earthquakes, *Ann. Rev. Earth Planet. Sci.,* **17**, 227-254.

Frohlich, C., R.J. Willemann (1987). Aftershocks of deep earthquakes do not occur preferentially on nodal planes of focal mechanisms, *Nature,* **329**, 41-42.

Goldstein, P. and S. Jarpe (1994). Comparison of chemical and nuclear-explosion source spectra from close-in, local, and regional seismic data, *Proceedings of the Symposium on The Non-Proliferation Experiment: Results and Implications for Test Ban Treaties,* April 19-21, 1994, M.D. Denny, ed., Rockville, MD, CONF-9404100, 6-98 - 6-106.

Fliedner, M.M., S. Ruppert, and the Southern Sierra Nevada Continental Dynamics Working Group (1996). Three-dimensional crustal structure of the southern Sierra Nevada from seismic fan profiles and gravity modeling, *Geology,* **24**, 367-370.

Hannon, W.J. (1994). The Non-Proliferation Experiment, *Proceedings of the Symposium on The Non-Proliferation Experiment: Results and Implications for Test Ban Treaties,* April 19-21, 1994, M.D. Denny, ed., Rockville, MD, CONF-9404100, 2-1 - 2-11.

Hearn, T., N. Beghoul, and M. Barazangi (1991). Tomography of the Western United States from regional arrival times, *J. Geophys. Res.*, **96**, 16,369-16-381.

Kirby, S.H., W.B. Durham, and L.A. Stern (1991). Mantle phase changes and deep-earthquake faulting in subducting lithosphere, *Science,* **252**, 216-224.

Lawson, J.E. (1994). Catalog of known and putative nuclear explosions from unclassified sources, *http://www.pal.xgw.fi/hew/catalog.*

McCormack, D.A., K.F. Priestley, H.J. Patton (1994). Distance effects on regional discriminants along a seismic profile in northwest Nevada; NPE and nuclear results, *Proceedings of the Symposium on the Non-Proliferation Experiment: Results and Implications for Test Ban Treaties,* April 19-21, 1994, M.D. Denny, ed., Rockville, MD, CONF-9404100, 6-254 - 6-255.

Myers, S., T. Wallace, S. Beck, P. Silver, G. Zandt, J. Vandecar, and E. Minaya (1995). Implications of spatial and temporal development of the Mw=8.3 June 9, 1994 deep Bolivia earthquake sequence,*Geophys. Res. Lett.*, **22**, 2269-2272.

Panel on seismological research requirements for a Comprehensive Test-Ban monitoring system (1995). *Seismological Research Requirements for a Comprehensive Test-Ban Monitoring System,* National Academy Press.

Parsons, T, J. McCarthy, W.M. Kohler, C.J. Ammon, H.M. Benz, J.A. Hole, and E.E. Criley (1996). Crustal structure of the Colorado Plateau, Arizona: Application of new long-offset seismic data analysis techniques, *J. Geophys. Res.*, **101**, 11,173 - 11,194.

Parsons, T. (1995). The Basin and Range Province in *Continental Rifts: Evolution, Structure, Tectonics, Developments in Geotectonics 25*, edited by K.H. Olsen, Elsevier, Amsterdam, 277-324.

Pomeroy, P.W., W.J. Best, and T.V. McEvilly (1982). Test ban treaty verification with regional data - a review, *Bull. Seism. Soc. Am.*, **72B**, S89-S129.

Randall, G.E. (1994). Efficient calculation of complete differential seismograms for laterally homogeneous earth models, *Geophys. J. Int*, **118**, 245-254.

Richards, P.G. and J. Zavales (1995). Seismological methods for monitoring a CTBT: The technical issues arising in early negotiations, in *Monitoring a Comprehensive Test Ban Treaty*, E.S. Husebye and A.M. Dainty eds.

Saltus, R.W., and G.A. Thompson (1995). Why is it downhill from Tonopah to Las Vegas?: A case for mantle plume support of the high northern Basin and Range, *Tectonics*, **14**, 1235-1244.

Schultz, C.A., S.C. Larsen, P. Goldstein, and S.D Ruppert (1995). Wave-propagation modeling capabilities at LLNL: Applications to regional discrimination, *Proceedings of the 17th Seismic Research Symposium on Monitoring a Comprehensive Test Ban Treaty*, September 12-15, 1995, J.F. Lewkowicz, J.M. McPhetres, and D.T Reiter, eds., Scottsdale, AZ, PL-TR-95-2108, 504-513.

Schwartz, S.Y. (1995). Source parameters of aftershocks of the 1991 Costa Rica and 1992 Cape Mendocino, California, earthquakes from inversion of local amplitude ratios and broadband waveforms, *Bull. Seism. Soc. Am.*, **85**, 1560-1575.

Silver, P.G., S.L. Beck, T.C. Wallace, C. Meade, S.C. Myers, D.E. James, and R. Kuehnel (1995). The rupture characteristics of the great, deep Bolivian earthquake of 1994 and the physical mechanisms of deep-focus earthquakes,*Science*, **268**, 69-73.

Taylor, S.R., N.W. Sherman, and M.D. Denny (1988). Spectral discrimination between NTS explosions and western United States earthquakes at regional distances, *Bull. Seism. Soc. Am.*, **78**, 1563-1579.

Taylor, S.R., M.D. Denny, E.S. Vergino, and R.E. Glaser (1989). Regional discrimination between NTS explosions and western U.S. earthquakes, *Bull. Seism. Soc. Am.*, **79**, 1142-1176.

U.S. Congress, Office of Technology Assessment, (1988). *Seismic Verification of Nuclear Testing Treaties*, OTA-ISC-36, Washington, DC: U.S. Government Printing Office.

van der Vink, G.E., D.W. Simpson, C.B. Hennett, J. Park, T. Wallace (1994). *Nuclear Testing and Nonproliferation: The role of seismology in deterring the development of nuclear weapons*, The IRIS Consortium, February.

Wallace, T.C., M.A. Tinker, S. Myers, J. Swenson, R. Brazier, G. Fan, S. Beck, and G. Zandt (1994). Introduction: DOE Non-Proliferation Experiment, *Arms Control and Nonproliferation Technologies,* DOE/AN/ACNT-94A, First Qtr., 61.

Walter, W.R., K.M. Mayeda, and H.J. Patton (1994). Regional seismic observations of the Non-Proliferation Experiment at the Livermore NTS network, *Proceedings of the Symposium on the Non-Proliferation Experiment: Results and Implications for Test Ban Treaties,* April 19-21, 1994, M.D. Denny, ed., Rockville, MD, CONF-9404100, 6-193 - 6-201.

Walter, W.R., K.M. Mayeda, and H.J. Patton (1995). Phase and spectral ratio discrimination between NTS earthquakes and explosions. Part I: empirical observations, *Bull. Seism. Soc. Am.,* **85**, 1050-1067.

Wessel, P., and W.H.F. Smith (1991). Free software helps map and display data, *EOS Trans. Amer. Geophys, U.,* 72, 441, 445-446.

Wiens, D.A., J.J. McGuire, P.J. Shore, M.G. Bevis, K. Draunidalo, G. Prasad, and S. Helu (1994). The aftershock sequence of a large deep earthquake, *Nature,* **372**, 540-542.

Willemann, R.J. and C. Frohlich (1987). Spatial patterns of aftershocks of deep focus earthquakes, *J. Geophys. Res.,* **92**, 13,927-13,943.

Wu, J., T.C. Wallace, S.L. Beck, A very broad band study of the deep Bolivia earthquake sequence, submitted to *Geophys. Res. Lett.*, 1995.

Zandt, G., Myers, S.C., and Wallace, T.C. (1995). Crust and mantle structure across the Basin and Range-Colorado Plateau boundary at 37° N latitude and implications for Cenozoic extensional mechanism, *J. Geophys. Res.*, **100**, 10,529-10,548.